Contract Report

Continued Evaluation of Potential for Geologic Storage of Carbon Dioxide in the Southeastern United States

By:
Rebecca C. Smyth, David L. Carr, Susan D. Hovorka,
Stuart Coleman, Caroline Breton, and Erin N. Miller

prepared for:
Southern States Energy Board
Duke Energy
Santee Cooper Power
Southern Company

Gulf Coast Carbon Center
Bureau of Economic Geology
Scott W. Tinker, Director
Jackson School of Geosciences
The University of Texas at Austin

October 2011

Table of Contents

List of Tables

List of Figures

List of Plates

Executive Summary

The need to reduce atmospheric emissions of carbon dioxide (CO2) from industrial sources is now recognized internationally. As a result, companies operating coal-fired and other types of power plants in the southeastern U.S. (SE US) have been seeking information on the potential for long-term storage of CO2 in nearby subsurface geologic formations. Previous studies have shown there to be little to no capacity for onshore subsurface storage of CO2 in deep saline reservoirs in the Carolinas and northern Georgia (GA) (Smyth et al., 2008). However prior to this study, southern GA had not been assessed for geologic sequestration (GS) capacity potential. It is currently not known if extensive petroleum reserves exist below the continental shelf of the Atlantic Ocean offshore from SE US but, potential offshore capacity for storage of CO2 is large.

The objectives of this study have been to (1) assess the potential for GS of CO2 in areas of SE US not previously characterized (i.e. southern GA coastal plain between the panhandle of Florida (FL) and the Atlantic Ocean) and (2) refine capacity estimates for portions of offshore geologic units present below the nearby Atlantic continental shelf. We primarily focused on geographic areas where CO2 can be stored in deep saline reservoirs at depths great enough to keep it in supercritical phase, but also had to consider surrounding areas in order to better solve the geological puzzle. Maintaining CO2 in supercritical phase requires temperature greater than 31.1 °C (88 °F) and pressure greater than 7.39 MPa (72.9 atm), which corresponds to depth below ground surface of ~800 m (2600 ft). Results of this detailed study of the regional subsurface geologic units are timely for operators of coal-fired power plants in the SE US because technologies to separate, capture, and concentrate CO_2 from industrial emissions are ready for commercial-scale demonstration.

Two areas with thick accumulations of coastal plain sediment underlie the southwest and southeast GA embayments. It is in thicker sections of the embayments, both onshore and offshore, that nonmarine, clastic (i.e., gravel-, sand-, and silt-bearing) strata have the highest potential for deep geologic storage of CO2 generated in the SE US.

To battle the complexity of Georgia's deep subsurface geology, Carr used the concepts of sequence stratigraphy to define the large-scale distribution of two potential CO_2 geologic sequestration units (GSUs). The sequence stratigraphic method focuses on tracing correlative time surfaces in cross sections that are made up of individual well logs and/or descriptions of rock core collected from wellbores. The advantage of the sequence stratigraphic method is that applied correctly, it captures architecture of rock units more accurately and at scales that affect subsurface fluid flow. After many iterations of correlation and cross section construction, Carr identified the following major stratigraphic packages within our area of interest:

1. Pre-Tuscaloosa sandstones/conglomerates of upper Jurassic (?) to Early Cretaceous age
2. Tuscaloosa (or equivalents) sandstones of early Late Cretaceous-age
3. Post- Tuscaloosa sandstones and limestones of Late Cretaceous age

The two intervals with sufficient thicknesses of net permeable clastic strata, at depths deep enough to store CO2 in supercritical phase, are Pre-Tuscaloosa and Tuscaloosa (fig. 1).

Estimates for the capacity of subsurface geologic units to store CO2 depend on, among other variables, the thickness of permeable sand present in a reservoir. We estimated CO2 storage capacity of the two GSUs by (1) establishing geologic framework and determining porosity in Petra geologic modeling software (2) exporting data to ArcGIS, and (3) using the

methodology developed primarily by researchers at the Massachusetts Institute of Technology (MIT, 2010) and reported in the U.S. Department of Energy, National Energy Technology Laboratory National Carbon Sequestration Atlas (NETL, 2010) for saline reservoir capacity

The total capacity for the Pre-Tuscaloosa GSU, using an efficiency factor (E) of 2 percent, is ~111 Gt over an area of ~74,000 mi^2 (191,000 km^2). The total capacity for GS of CO2 in the Tuscaloosa GSU, using E = 2 percent, is ~31 Gt over an area of ~65,000 mi^2 (168,000 km^2). Areas with higher capacity are in offshore portions of the SW and SE GA embayments, which is where the thickest accumulations of permeable sands and highest estimated porosities lie.

Introduction

The need to reduce atmospheric emissions of carbon dioxide (CO2) from industrial sources, especially coal-fired power plants, is now recognized internationally. As a result, companies operating coal-fired and other types of power plants in the southeastern United States (SE US) have been seeking information on the potential for long-term storage of CO2 in nearby subsurface geologic formations. Deep subsurface geologic storage (GS) of CO2 will take place in two types of settings (1) oilfields undergoing enhanced oil recovery (EOR) using CO2 and (2) saline reservoirs in which CO2 will be stored, albeit without the added benefit of revenues from increased oil production. In both types of settings, CO2 will be injected into geologic units that are deeper than, and isolated from, underground sources of drinking water.

Previous workers (primarily the Georgia and United States geological surveys) have documented that the onshore areas of interest in this study lack petroleum reserves, hence there are no potential EOR fields. Previous studies have also shown there to be little to no capacity for onshore subsurface storage of CO2 in deep saline reservoirs in the Carolinas and northern GA (figure 1). However prior to this study, southern GA had not been assessed for GS capacity potential. It is currently not known if extensive petroleum reserves exist below the continental shelf of the Atlantic Ocean offshore from SE US but, potential offshore capacity for storage of CO2 is large.

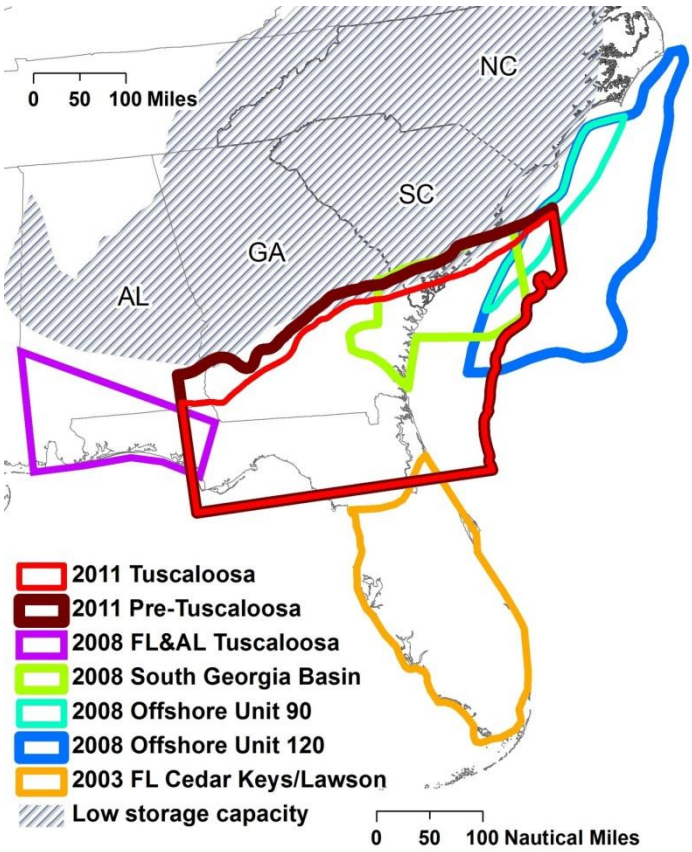

Figure 1. Potential CO2 geologic sequestration areas along coastal plains of the southeastern U.S.

An advantage of siting CO2 storage operations in oil producing areas is that there is much information on the subsurface geologic formations into which CO2 can be injected. However a risk associated with oilfield injection of CO2 is the economic disadvantage of having to plug abandoned or damaged wells to keep the CO2 from escaping back up to the surface and into the atmosphere. One advantage of siting CO2 storage operations in offshore settings is that the risk of impacting overlying drinking water resources is removed. For much of the SE US where onshore capacity to store CO2 in geologic strata is limited, the best options may be offshore. Reasons for this are large GS storage capacity in strata thousands of feet below the seafloor, and the absence of wells drilled through seals (i.e. low permeability geologic strata) that would impede migration of CO2 from deep injection zones up to the seafloor.

Previous studies of capacity for storage of CO2 in the SE US were conducted on a reconnaissance level and relied primarily on previously published work for information. Results of this detailed study of the regional subsurface geologic units are timely for operators of coal-fired power plants in the SE US because technologies to separate, capture, and concentrate CO_2 from industrial emissions are ready for commercial-scale demonstration.

In a previous "Carolinas report", Smyth et al. (2008) identified areas (e.g., 2008 areas on fig. 1) potentially suitable for long term GS of up to 250 gigatons (Gt) of CO2 in the SE US onshore and offshore Atlantic deep subsurface. This study was funded by companies operating power plants in the SE US: Duke Energy, Progress Energy, Santee Cooper Power, and South Carolina Electric and Gas, in cooperation with the Electric Power Research Institute (EPRI) and the Southern States Energy Board (SSEB).

The 2008 Carolinas study updated and superseded previous CO2 source-sink matching studies (Hovorka et al., 2000, 2003) of the SE US (e.g., 2003 area on fig. 1). This Southeast Regional Carbon Sequestration Partnership (SECARB) Phase I reconnaissance-level capacity-estimation study was funded by the Department of Energy (DOE) National Energy Technology Laboratory (NETL) and administered by SSEB.

In the current study: *Continued Evaluation of Potential for Geologic Storage of Carbon Dioxide in the Southeastern United States*, Gulf Coast Carbon Center (GCCC) personnel at the Bureau of Economic Geology (BEG), Jackson School of Geosciences (JSG), The University of Texas at Austin (Carr and Coleman), with assistance from SSEB, assembled a geologic database of borehole geophysical logs (logs) and depth picks for geological stratal markers. Carr then correlated geologic strata and identified nonmarine, clastic (i.e., gravel-, sand-, and silt-bearing) units suitable for CO2 subsurface storage (2011 areas on fig. 1). The stratigraphic correlations have been more difficult than similar past and current studies conducted in the central and western Gulf of Mexico because of relative paucity of detailed geological data and complexities associated with plate tectonic history of the region.

The objectives of this study have been to (1) assess the potential for GS of CO2 in areas of SE US not previously characterized (i.e. southern Georgia (GA) coastal plain between the panhandle of Florida (FL) and the Atlantic Ocean) and (2) refine capacity estimates for portions of offshore geologic units present below the nearby Atlantic continental shelf. To accomplish these objectives we concentrated on an area within the Gulf of Mexico and Atlantic coastal plains of southeastern Alabama, northern FL, and southern GA, and below the continental shelf of the Atlantic Ocean offshore from northern FL, GA, and southern South Carolina (SC). We primarily focused on geographic areas where CO2 can be stored in deep saline reservoirs at depths great enough to keep it in supercritical phase, but also had to consider surrounding areas in order to better solve the geological puzzle.

Regional Geologic Setting and Geologic History

Assembly of a geologic model, through correlation of stratigraphic units in the onshore/offshore subsurface of the southeastern U.S., has been complicated by movement of tectonic plates over geologic time (see Appendix I - Geologic Time Scale). The breakup and reassembly of continental masses and seafloor spreading have resulted in fragments of earth's crust (igneous, sedimentary, and metamorphic rocks) being attached to different continents at different times in the past. Relevant periods of plate tectonic history of our region of interest are shown in fig. 2. These images of global distribution of continents are from the PLATES project at The University of Texas at Austin Institute of Geophysics (UTIG) (Dalziel, 1995, 1997, 2000; Dalziel et al., 2000; and UTIG, 2011). Here we show three examples of many available reconstructions of earth's continents over a 750 million year (Ma) timespan. The geologic time periods represented in fig. 2 are 320 Ma (early Pennsylvanian), 180 Ma (middle Jurassic), and 100 Ma (middle Cretaceous).

In early Pennsylvanian time much of the study area was positioned between the northeastern continental U.S. and northwestern Africa (orange area with Floridian peninsula in fig. 2a). More recently (middle Jurassic time) the region became attached to the North American continent in its current configuration, with northern Africa attached to the northeast (fig. 2b). This large mass of continents is referred to as the super continent, Pangaea. The present day

Appalachian Mountains were uplifted during continental collisions that formed Pangaea. Rocks of the ancestral Appalachian Mountains terminate abruptly in GA because this was the southern edge of the North American continent at that time (e.g., Nelson et al., 1989).

By early Mesozoic (Triassic to early Jurassic time), seafloor spreading (black lines in fig. 2c) in the mid-Atlantic was underway; during this time the North American continent was moving westward away from Africa and South America (a continental mass called Gondwana) and the Gulf of Mexico was opening up. Breakup of Pangaea also resulted in formation of rift basins (tears in the continental crust) concentrated in areas of crustal weakness resulting from previous continental collision (i.e., FL, southern GA, and parts of SC becoming part of the North American continent). The yellow-shaded area on fig. 3 is a *zone* of early Mesozoic rift basins that trend northeast-southwest across southern AL/southern GA/northern FL/southern SC, and extend underneath the Atlantic seafloor.

Also shown in figure 3 is a feature called the Fall Line. This is an erosional boundary separating the Piedmont physiographic province of the Appalachian Mountains from the coastal plain. Fractured crystalline metamorphic rocks like those exposed in the Piedmont underlie landward portions of the GA coastal plain (e.g., Dillon et al., 1979). As concluded in Smyth et al. (2008), rocks of the Piedmont province and western portions of the coastal plain are not suitable for GS of CO2. The coastal plain sedimentary strata of Cretaceous and Tertiary age begin at the Fall Line and thicken seaward to, and beyond, the present-day continental shelf edge located approximately 80 miles offshore.

a

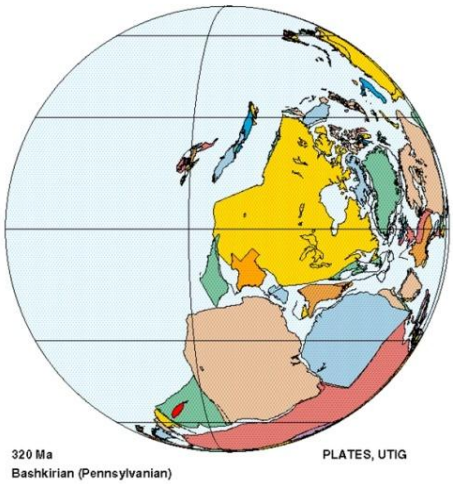

b

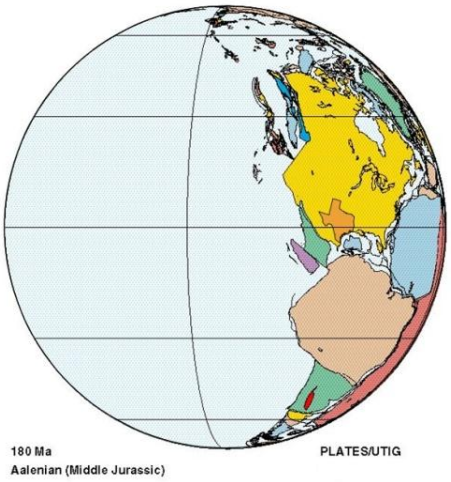

c

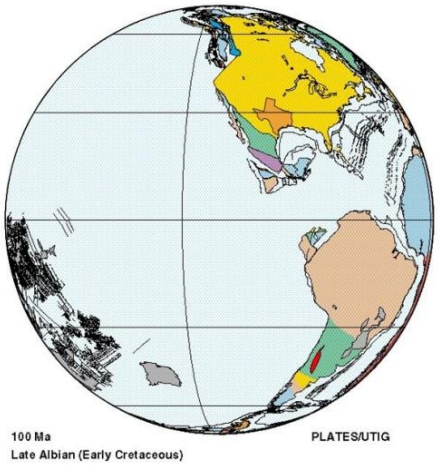

Figure 2. Plate tectonic reconstructions for (a) Pennsylvanian (320 Ma), (b) Middle Jurassic (180 Ma), and (c) Early Cretaceous (100 Ma) geologic time periods.

Two areas with thick accumulations of clastic sediment lie on the eastern and western ends of the early Mesozoic age rift zone that is buried beneath coastal plain sediments (Marine and Simple, 1974). The sedimentary basin on the western side has been given various names by multiple authors: southwest Georgia embayment, Tallahassee graben, and Apalachicola embayment; the basin on the east has primarily been referred to as the southeast Georgia embayment, but has also been called the Okeefenokee embayment and the Savannah basin. In this report we refer to these basins as the southwest and southeast Georgia embayments. Axes along the thickest portions of these embayments are shown as black lines with converging arrows (fig. 3). Sediment filling the basins came from the Appalachian Mountains to the north and northwest (e.g., Applin and Applin, 1944; King, 1959; McBride et al., 1989) and "southern highlands" (Chowns and Williams. 1983). According to Maher and Applin (1971); Popenoe and Zietz (1977), Nelson et al. (1985), the GA embayments are situated over early Mesozoic rift basins so they received a greater thickness of sediment than intervening areas that were topographically higher at the time.

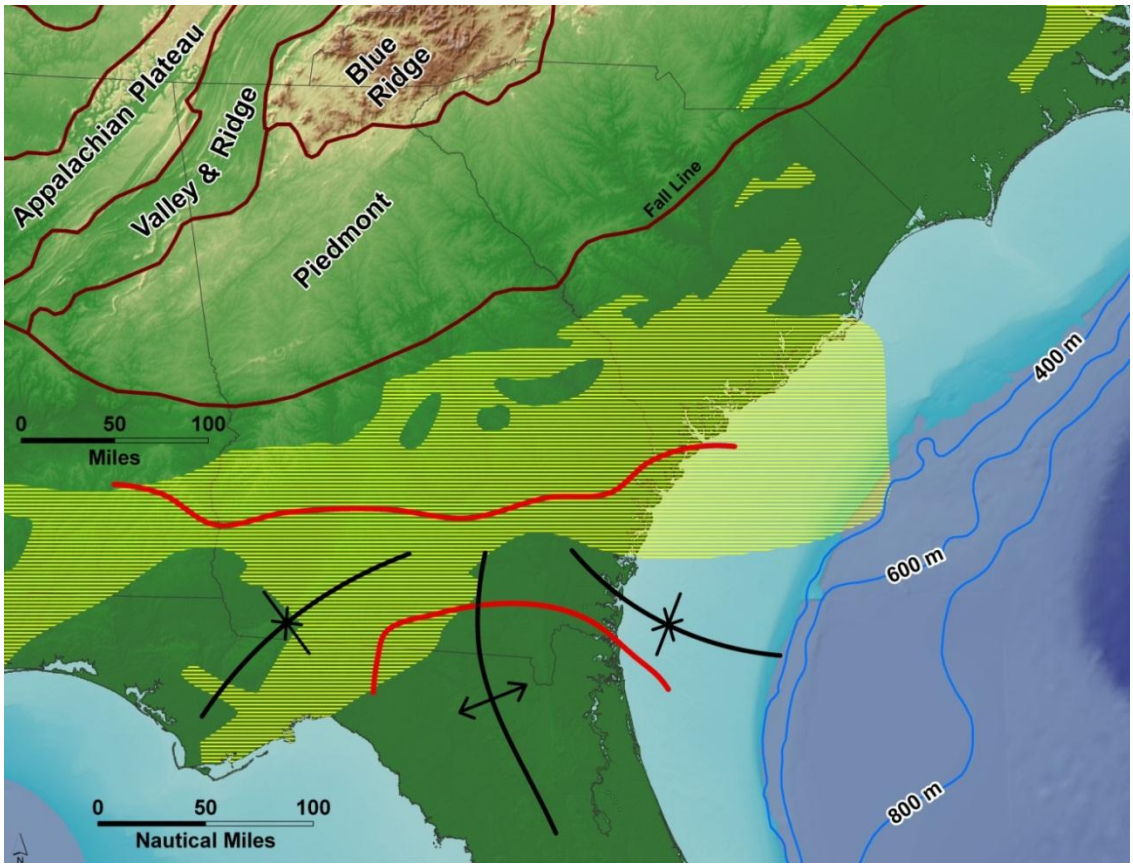

Figure 3. Regional geologic and physiographic setting. Structural features shown include (1) Appalachian Mountain provinces: Appalachian Plateau, Valley and Ridge, Blue Ridge, and Piedmont, (2) Early Mesozoic period rift basin in yellow stripes, (2) Central Georgia Uplift/Pennisular Arch in Florida (black line with diverging arrows); (3) Southwest and Southeast Georgia embayments (black lines with converging arrows), and (4) Suwannee saddle (outlined in red). Map features modified from: Fenneman and Johnson (1946); Klitgord and Behrendt (1979); Frazier and Schwimmer (1987)Olsen et al. (1991); Hutchinson et al. (1997); and constructed during this study. Digital elevation models from NOAA (2006) (land) and Scripps (2006) (ocean floor).

The thickest accumulations of sediment in the embayments, as defined by the black axes in this study, do not exactly correspond with published locations of the rift basins (fig. 3). Reasons for this difference are discussed further in the results sections below. The embayments are not continuous across southern GA because a structural high, the central Georgia uplift in GA and the Pennisular Arch in FL lies between them (e.g., Frazier and Schwimmer, 1987). The axis of this uplifted area is shown as a black line with diverging arrows (fig. 3). This region has been elevated relative to the embayments since at least early Mesozoic as can be deduced from the basement structure map (fig. 4), and probably arose during early Mesozoic rifting as suggested by Smith (1982).

The updip limits of the GA embayments and the FL-GA arch are centered on a structural/stratigraphic feature called the Suwannee saddle (named by Applin and Applin, 1965; red lines in fig. 3; called Suwannee strait by others). This feature, which lies on the northern edge of the Suwannee basin of northern FL (as defined by Smith, 1982), is coincident with the late Paleozoic suture zone between North America and Africa (Chowns and Williams, 1983, fig. 12). To call the Suwannee basin a basin is confusing if you are only looking at surfaces of Mesozoic and younger rocks (figs. 4, 11, 12, 15), especially since the FL peninsular arch runs almost through the middle of it (Smith, 1982). But rocks of the Suwannee basin are composed of older, early Paleozoic age, flat-lying sedimentary strata that were deposited in deep water along a continental margin (i.e. a basin) located south of the present day Suwannee saddle (fig.3). These Paleozoic strata and underlying high-silica igneous rocks are more similar to Africa than they are to North America (e.g., Applin, 1951; Barnet, 1975, Smith, 1982); hence they have no correlative units to the north.

More recent Mesozoic strata that overlie rocks of the Suwannee basin are too shallow to serve as potential GSUs. In addition, after early Cretaceous time carbonate sedimentation dominated the southern high (Pennisular Arch) whereas primarily terrigenous clastic units were deposited to the north. By upper Cretaceous time the Atlantic shoreline was at least as far west as the Fall Line (fig. 3, Frazier and Schwimmer, 1987); hence most rocks of this age are carbonates (Applin and Applin, 1944; Buffler et al., 1979). It is in thicker parts of the lower Cretaceous and older strata that the highest potential for GS of CO2 generated in SE US exists, both onshore and offshore.

Methodology

To battle the complexity of Georgia's deep subsurface geology, Carr used the concepts of sequence stratigraphy to define the large-scale distribution of potential CO_2 geologic sequestration units (GSUs). The sequence stratigraphic method focuses on tracing correlative time surfaces in cross sections that are made up of individual well logs and/or descriptions of rock core collected from wellbores (e.g. data point locations on fig. 4). This approach is different from more traditional methods of mapping geologic strata, which typically transgress time. The advantage of the sequence stratigraphic method is that applied correctly, it frequently captures architecture of rock units more accurately and at scales that affect subsurface fluid flow.

Note that the map areas outside those covered by the cross sections (fig. 4) are populated with data from published maps and geologic picks of stratal surfaces (i.e. tops and bottoms of regionally recognized geologic units). For example, in offshore areas where there are long distances between data points, we used a published map of depth to basement (Klitgord and

Behrendt, 1979) to aid construction of our basement map, which covers both offshore and onshore regions. We then used our basement map to aid stratigraphic correlation of units in areas without geophysical logs.

Stratigraphic correlations were accomplished through construction of seven regional cross sections, A-A' through G-G' (fig. 4). The method was to correlated key stratigraphic surfaces defining major reservoir packages, and then correlated additional wells using the nearest cross section wells as type logs. By constructing multiple cross sections in orthogonal directions Carr was able to double check correlations of geological strata at crossing points along the sections and interpret depositional patterns along dip and strike orientations.

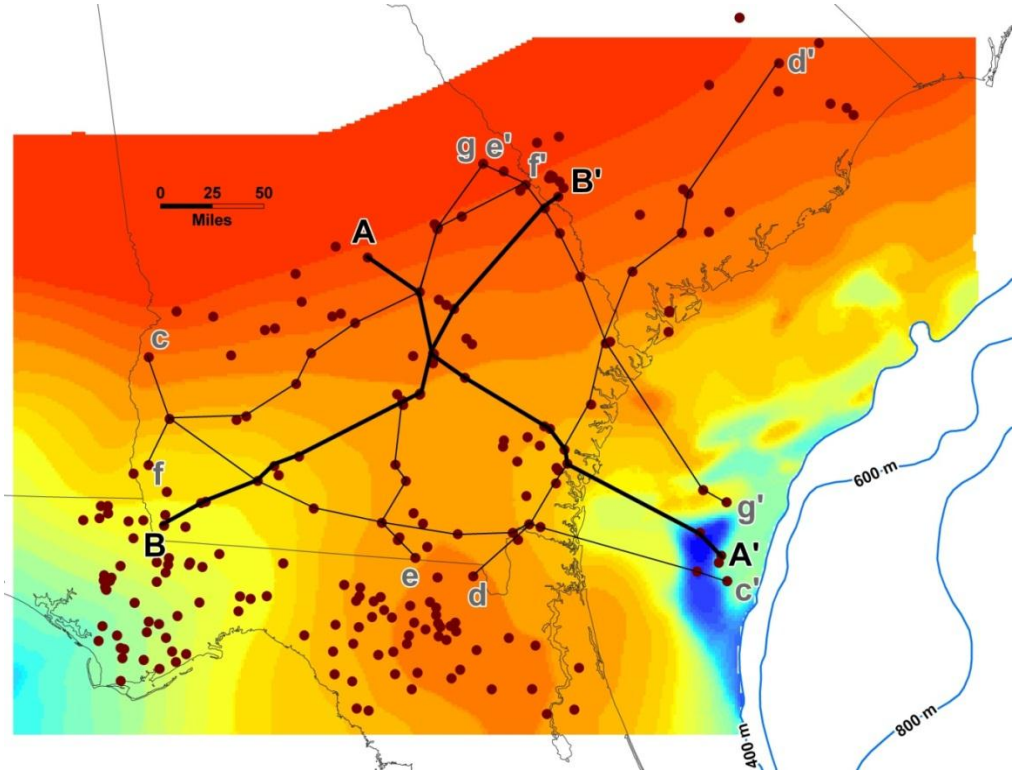

Figure 4. Locations of data points and geologic cross sections superimposed on structure contour map of depth to basement rocks. Red to orange depth range = 200-5,000 ft below sea level (bsl). Yellow to dark blue depth range = 5,000 to 25,000 ft bsl. Offshore bathymetric contours in meters (blue lines).

Steps used by GCCC researchers to (1) construct the digital geologic model, (2) characterize reservoir properties of lithology, porosity, and permeability, and (3) calculate capacity for geologic storage of CO2 were as follows:

a) Compiled and reviewed geophysical log data, published literature, and maps
b) Constructed digital data base of logs, geophysical data, and pre-existing maps using IHS Petra© software
c) Performed sequence stratigraphy-based interpretation to define gross reservoir architecture, which included construction of cross sections.
d) Selected geological sequestration units (GSU) stratigraphic intervals: Pre-Tuscaloosa and Tuscaloosa
e) Mapped structure of top of basement, Pre-Tuscaloosa, Tuscaloosa Fm., and upper Cretaceous surfaces

f) Mapped structure of base of Tuscaloosa and upper Cretaceous surfaces
g) Made isopach maps of Pre-Tuscaloosa, Tuscaloosa, and upper Cretaceous intervals
h) Performed cursory petrophysical analysis on well log curves to define permeable net sandstone and average porosity for GSU intervals
i) Performed reservoir summation to count permeable net sandstone and determine average porosity within sand units for GSU intervals
j) Mapped permeable net sandstone and average porosity for GSU intervals
k) Converted structure contours of depth below ground surface for each GSU, by adding surface elevation to depth below sea level grids.
l) Calculated CO2 densities at midpoint depths for each GSU strata within suitable depth intervals
m) Calculated capacity for CO2 in net sands for each GSU and compiled results in ESRI ArcGIS© software using the method of MIT and NETL (2010).

Below we describe in detail the sources of data, and methodologies used to (1) interpret reservoir properties from different types of logs (2) construct multiple types of maps, and (3) define GSUs.

Data sources

Since there has been no hydrocarbon production in the state of Georgia, a large, high-quality subsurface data base was not readily available. Hence, we gathered and integrated data from a wide variety of sources, including research boreholes, water wells, and petroleum exploration wells. In addition, we relied upon core descriptions and previously published works to calibrate our interpretations and fill in data gaps, especially offshore. Sources of published work of particular usefulness in geologic correlations were those of Herrick (1961), Applin and Applin (1964; 1967), Dillon et al. (1979), Gohn et al. (1980), and Poppe et al. (1995).

We collected and utilized well logs from 74 wells for making stratigraphic interpretations. Vector log curves (**L**og **A**scii **S**tandard commonly referred to as "LAS") were available for 30 of these wells, raster images for 68 wells, and we had both raster images and LAS curves for 22 wells. For mapping two key stratigraphic surfaces (top of Cretaceous, top of basement) that bound the majority of potential GSUs, we also utilized IHS Energy geologic formation top picks from 157 additional wells. Locations of all log and core data points are shown on fig. 3.

Geophysical logs used to construct a geologic model for this project came from:

- A compilation of logs from the former Georgia Geological Survey files, an effort previously funded by Southern Company
- Additional former Georgia Geological Survey logs acquired by SSEB
- IHS database commercial library of geophysical logs and geological formation picks
- A2D Technologies commercial log library
- BEG log library

Multiple sets of offshore geophysical and stratigraphic data were previously collected primarily from ocean-going research vessels, and some from aircraft, by multiple research institutions/consortia during the 1970s and early 1980s:

- United States Geological Survey
- The University of Texas Marine Science Institute

- Continental Offshore Stratigraphic Test program
- Deep Sea Drilling Project
- Institut Francais du Petrole

The types of geophysical data sets include:

- Single- and multi-channel seismic reflection profiles
- Seismic refraction profiles
- Magnetic surveys
- Free air and isostatic gravity surveys
- 2-D gravity and magnetic models
- Side-scan sonar

Many documents (maps, regional cross sections, reports, and published articles) have been produced from analyses of these offshore data sets, primarily by USGS researchers, but also from academic institutions. Previous interpretations of onshore geological data came from the Georgia Geological Survey, academic institutions, and a minor amount from industry researchers.

Geophysical log interpretation

Many types of information about rocks in the subsurface can be extracted from borehole geophysical logs including lithology, porosity, and permeability. These properties control the distribution and movement of fluids in the subsurface. It is easier to predict how fluids will move through clastic rocks (i.e. those composed primarily of gravel, sand, silt, and clay) than carbonates, where fluid movement is usually dominated by conduit flow (along fractures or other curvilinear features in the rocks). Emphasis is being placed on clastic reservoirs for GS of CO2 because of the higher level of confidence with which fluid movement can be predicted. This applies to international geologic carbon sequestration projects and those being conducted in the U.S.

Clastic rock units that serve as effective subsurface fluid reservoirs are contain sandstones with high porosity and permeability. Since not all sandstones are conducive to fluid flow, it is important to identify net permeable sandstone units in order to more accurately estimate reservoir capacity. Quantitative description of reservoir rocks is conducted using petrophysical analysis of geophysical logs. We performed cursory petrophysical analysis on well log curves to estimate permeable net sandstone and average porosity.

Net sandstone estimates

We used spontaneous potential (SP) or gamma ray (GR) curves on geophysical logs to estimate net sandstone. SP provides the most useful estimate because it qualitatively indicates permeable sandstone. The GR curve is better than SP for estimating total sandstone volume; however, the GR does not differentiate between permeable and "tight" (impermeable) sandstones, which contain non-clay, pore-filling cements that diminish porosity and permeability. Because of this difference, SP curves were used where ever available to estimate net *permeable* sandstone in our analysis of CO_2 capacity.

There were two ways available to count net permeable sandstone from the available SP curves (1) direct interpretation from raster image curves (Fig. 5) and (2) automated summation from normalized vector curves (LAS; Fig. 6). In both cases, we used a guideline cutoff, beyond which, the SP deflection from a "shale base line" (Schlumberger, 1998, p. 3-5) was sufficiently negative to indicate permeable sandstone. A graphic comparison of these two methods is shown

in fig. 7. The cutoffs for the sand counts from raster log curves were more subjective than those for the LAS curves because SP readings directly from raster images are non-normalized. Hence the interpreter must choose a cutoff or even multiple cutoffs within a given well, such that most of the obvious permeable sandstone can be differentiated from the impermeable rocks below the "shale base line" (Schlumberger, 1998). Further, the cutoff line was used as a guide rather than a strict quantitative boundary, since the tops and bases of individual sandstone beds are marked by inflection points in the curves, which are typically close to a given cutoff, but frequently not exactly aligned with them and depend upon bed thickness (e.g., Schlumberger, 1998, p. 3-4, Fig. 3-3).

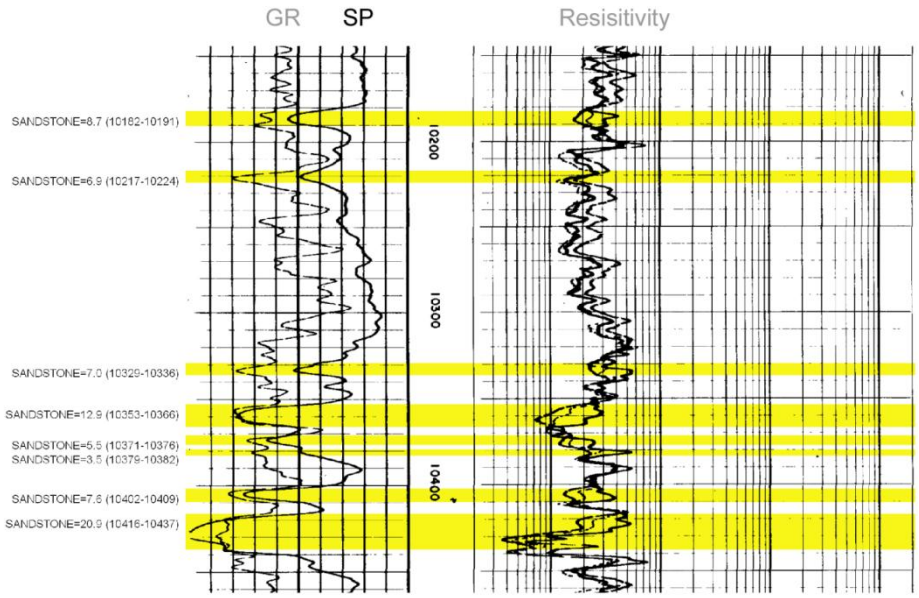

Figure 5. Example raster geophysical log image showing net permeable sandstone interpretations (yellow highlight). SP curve is solid in left hand track; GR curve is dashed. Annotations on far left show footage of net sandstone (and depths) for each interval. Total net permeable sandstone shown in this figure is 73.0 ft (equals the sum of the footages). Note that while SP and GR curve shapes mimic each other, the permeable sandstone as indicated by the SP is a subset of the total sandstone indicated by the GR.

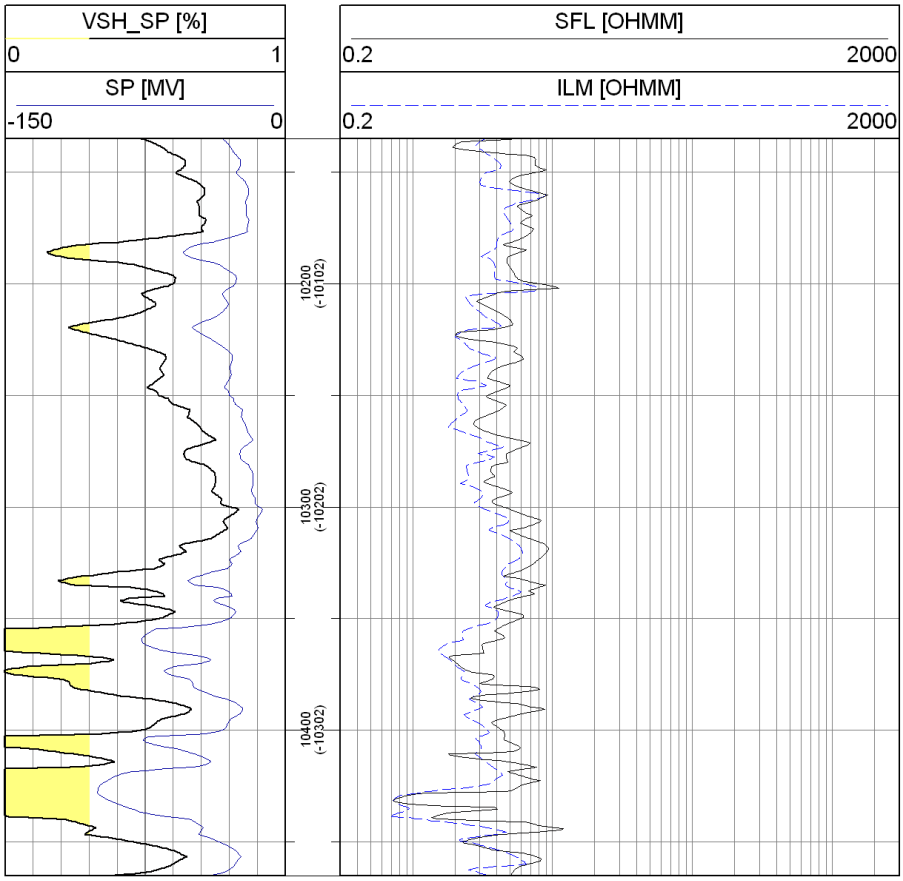

Figure 6. Example vector geophysical log (LAS) showing net permeable sandstone interpretations (yellow highlight) derived from SP curve. SP is solid blue curve in left hand track and VSH_{SP} curve is solid black curve with <30% shale volume cutoff applied indicating net permeable sandstone. Total net permeable sandstone (sum of yellow-highlighted intervals in VSH_{SP} curve) shown in this figure is 78.5 ft. Right-hand track shows SFL and ILM resistivity curves.

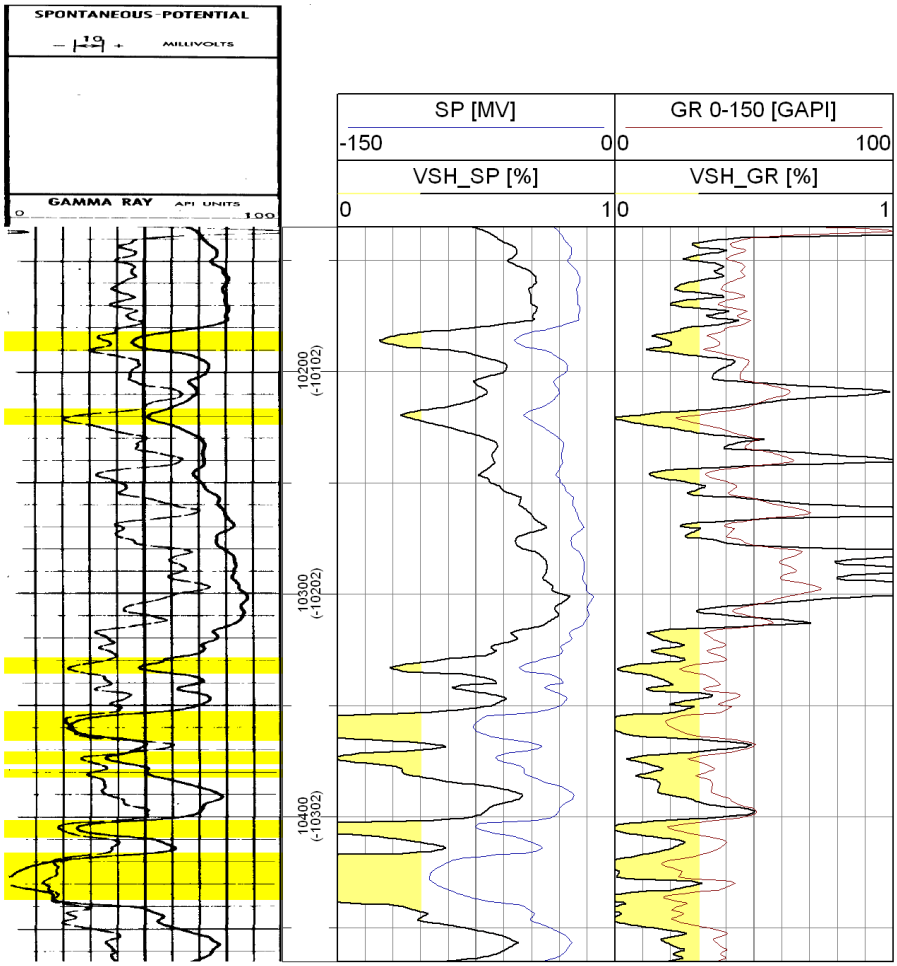

Figure 7. Comparison of net sandstone estimates from raster-SP (left track), and vector log (LAS) computations from SP (VSH_SP; middle track) and GR (VSH_GR; right track). VSH_SP and VSH_GR curves are solid black curve with <30% shale volume cutoff applied indicating net sandstone. Respective net sandstone estimates for SP-raster, SP-LAS and GR-LAS for this interval are 73.0 ft, 78.5 ft, and 173.0 ft.

The SP vector curves (LAS), were normalized by applying a "shale volume" model which converts the SP curve response into a shale percentage ranging from 0% to 100% after "100% clean sand" and "100% shale" parameters are defined:

Eqn. 1. $\mathbf{VSH_{SP} = (SP - SP_{CL}) / (SP_{SH} - SP_{CL});}$

Where,

$\mathbf{VSH_{SP}}$ = Shale volume from the SP curve
SP = SP curve reading (input)
$\mathbf{SP_{CL}}$ = SP reading in 100% clean sand (constant)
$\mathbf{SP_{SH}}$ = SP reading in 100% shale (constant).

Likewise, for the 11 wells lacking SP curves, the GR was substituted in a similar fashion (Eqn.'s 2 and 3), using a similar shale volume method, with the addition of the Clavier correction

(Asquith and Krygowski, 2004). Ten of these wells are located up dip from the 2,600-ft depth limits for CO_2 storage and were thus not critical to the accuracy of our capacity estimates.

Eqn. 2. $\mathbf{I_{GR} = (GR - GR_{CL}) / (GR_{SH} - GR_{CL});}$

Where,

$\mathbf{I_{GR}}$ = Gamma Ray Index: Intermediate calculation of shale volume from the GR curve
$\mathbf{GR_{CL}}$ = SP reading in 100% clean sand
$\mathbf{GR_{SH}}$ = SP reading in 100% shale.

Finally, the Clavier non-linear correction was applied:

Eqn. 3. $\mathbf{VSH_{GRc} = 1.7 - (3.38 - (VSH + 0.7)**2)**0.5;}$

Where,

$\mathbf{VSH_{GRc}}$ = Shale volume from the GR curve, corrected for overly optimistic non-linearity of Eqn. 2.

Based on visual inspection of $\mathbf{VSH_{SP}}$ and $\mathbf{VSH_{GRc}}$ logs, a cutoff of 30% was used to define net sandstone, i.e., a shale volume of less than 0.3 was deemed to indicate permeable sandstone.

Porosity estimates

Vector (LAS) porosity curves were available for 15 wells. Porosity estimates for ten (10) of the wells were based on sonic logs; the remaining five (5) wells were based on density porosity. Raster porosity logs were also available for additional wells, but due to time/cost constraints were not utilized for porosity mapping.

Sonic porosity was calculated using the empirically modified Wyllie time average equation (Wyllie, 1956; Alberty, 1994):

Eqn. 4. $PHIS = 0.67 * ((DT - DT_M) / (DT_{FL} - DT_M))$

Where,

PHIS = Sonic porosity
DT = Sonic log delta-t reading (input)
DT_M = Sonic delta-t constant for rock matrix (sandstone = 55.5 μ -sec/ft)
DT_{FL}= Sonic delta-t constant for fluid (salt water = 189 μ-sec/ft)

Density porosity was calculated using:

Eqn. 5. $PHID = (RHO_M - RHOB)/(RHO_M - RHO_{FL})$

Where,

PHID = Density porosity
RHOB = Bulk density log reading (input)
RHO_M = Bulk density of rock matrix (sandstone = 2.65 gm/cc)
RHO_{FL}= Bulk density of fluid (salt water = 1 gm/cc)

Reservoir summations

Using the results of the petrophysical analysis, summations of the feet net permeable sandstone and average porosity were made for wells from which data these were available. A summation is a count of the footage of a particular set of petrophysical characteristics that define the quality of a reservoir for a particular purpose. In this study, a high quality interval would be one having a large footage of net permeable sandstone with a high average porosity.

Net Sandstone summation

Using our interpretation platform, Petra, we were able to automate the counting of net permeable sandstone from both raster images and vector (LAS) log curves for each GSU. Table 1 lists the results of the net permeable sandstone counts and data sources for wells used in the study.

Porosity summation

Again, utilizing Petra, Carr was able to automate the determination of average porosity within the permeable sandstone units for each GSU. Specifically, the program was told to average only porosity values where net sandstone satisfied the 30% cutoff or footages defined by raster interpretations of net permeable sandstone. Table 2 shows the average porosity calculated within the net permeable sandstone intervals and porosity data sources for wells used in the study.

Table 1. Net permeable sandstone summations for wells used in study.

					TUSCALOOSA GSU		PRE-TUSCALOOSA GSU	
State	**County**	**Well Label**	**Operator**	**TD**	**Net Sandstone**	**Data Source**	**Net Sandstone**	**Data Source**
AC	BRUNSWICK	913-1	GETTY OIL COMPANY	7,000	4	RASTER-SP	1,004	RASTER-SP
AC	BRUNSWICK	1005-1	TRANSCO EXPL&PROD CO	11,635	0	LAS-SP	1,530	LAS-SP
AC	JACKSONVILLE	564-1	EXXON CORPORATION	12,863	15	RASTER-SP	1,657	RASTER-SP
AC	JACKSONVILLE	472-1	EXXON CORPORATION	7,578	0	RASTER-SP	248	RASTER-SP
AC	JACKSONVILLE	COST #GE-1	OCEAN PRODUCTION CO	13,254	0	LAS-SP	1,661	LAS-SP
AC	JACKSONVILLE	427-1	TENNECO OIL CO	7,472	23	RASTER-SP	307	RASTER-SP
AC	JACKSONVILLE	208-1	TENNECO OIL CO	7,760	0	RASTER-SP	263	RASTER-SP
FL	ALACHUA	JOSIE PARKER #1	TIDEWATER OIL CO	3,218	76	RASTER-SP	0	RASTER-SP
FL	BAKER	H L HUNT #1	HUNT OIL CO	3,348	39	RASTER-SP	0	RASTER-SP
FL	DIXIE	P C CRAPPS A-1	SUN OIL COMPANY	5,103	106	RASTER-SP	244	RASTER-SP
FL	SUWANNEE	J W TILLIS #1	SUN OIL COMPANY	3,568	65	RASTER-SP	12	RASTER-SP
FL	TAYLOR	BROOKS-SCANLON INC BLOCK 33 #1	GULF OIL CORP	5,243	61	RASTER-SP	16	RASTER-SP
GA	APPLING	Mrs. W. E. Bradley #1	WEATHERFORD J E ETAL / Felsenthal-Weatherford	4,098	419	RASTER-SP	36	RASTER-SP
GA	ATKINSON	Doster-Ladson E #1	Sun Oil Co.	4,296	369	RASTER-SP	33	RASTER-SP
GA	BROOKS	Rogers Sr. B- #1	HUGHES D E	3,850	315	RASTER-SP	72	RASTER-SP
GA	Burke	Millers Pond	GGS	859	61	RASTER-GR	0	RASTER-GR
GA	Burke	Girard Test	USGS	1,385	59	RASTER-GR	0	RASTER-GR
GA	CALHOUN	J. W. West #1	Sowega Minerals Exploration	5,265	148	RASTER-SP	832	RASTER-SP
GA	CAMDEN	Pennington Union Camp #1	Amoco Production Company	10,000	53	RASTER-SP	0	RASTER-SP
GA	Camden	J.A. Buie #1	California	4,969	190	RASTER-SP	120	RASTER-SP
GA	CAMDEN	Union Camp B-1	Pan American Petroleum Corp.	4,690	53	RASTER-GR	0	RASTER-GR
GA	CHARLTON	O.C. Mizell #1	PENNZOIL PRODUCNG CO / South Penn Oil Co.	4,577	117	RASTER-SP	20	RASTER-SP
GA	CLINCH	Lem Griffis #1	MAROTT G J ETAL / Luke Grace Drilling Co.	4,588	68	RASTER-SP	2	RASTER-SP
GA	CLINCH	Timber Products Co. #1	Wiley P. Ballard Jr.	4,282	220	RASTER-SP	59	RASTER-SP
GA	Coffee	Terrel Thurman #1	Carpenter Oil Company	4,130	178	RASTER-SP	102	RASTER-SP
GA	Colquitt	H. Parker #1	Houston Oil & Minerals Corp.	6,902	298	RASTER-SP	662	RASTER-SP
GA	CRISP	Cecil Pate #1	KERR-MCGEE CORP	5,010	222	RASTER-SP	601	RASTER-SP
GA	DECATUR	G.E. Dollar #1	Renwar Oil Corporation	4,995	396	RASTER-SP	469	RASTER-SP
GA	DODGE	B&L FARMS #1	ATLANTA GAS LIGHT CO	4,529	186	LAS-SP	618	LAS-SP
GA	DOOLY	H.E. Walton #1	DOOLEY OIL ASSOC /Georgia-Florida Drilling Co	3,748	189	RASTER-SP	494	RASTER-SP
GA	EARLY	Susie Wilson #1	EXXON CORPORATION	9,176	162	LAS-SP	1,139	RASTER-SP
GA	ECHOLS	Superior Pine Prod #3	Hunt Oil Co.	4,003	110	RASTER-SP	149	RASTER-SP
GA	GLYNN	Union Bag Camp Paper Co. No. ST-	Humble Oil & Refining Co.	4,632	57	RASTER-SP	15	RASTER-SP
GA	GLYNN	Union Camp #1	Pan American	4,439	199	RASTER-SP	0	RASTER-SP

GA	Glynn	Scott & Mead Timber #1	USGS / William K. Davis	4,516	191	RASTER-SP	0	RASTER-SP
GA	Glynn	Union Camp Corp #1	William K. Davis	8,468	213	LAS-SP	72	LAS-SP
GA	JEFF DAVIS	J.L. Sinclair No. 1	Chevron USA, Inc.	4,063	164	LAS-SP	140	LAS-SP
GA	Jeff Davis	A.P. Snipes et al. #1	Chevron USA, Inc.	11,470	212	LAS-SP	45	LAS-SP
GA	JEFF DAVIS	SNIPES A R #1	Chevron USA, Inc.	11,470	133	LAS-SP	50	LAS-SP
GA	Laurens*	Grace McCain #1	Calaphor MFG. Corp.	2,548	188	RASTER-SP	138	RASTER-SP
GA	LIBERTY	Jelks & Rodgers No.1	E.B. LaRue	4,254	388	LAS-SP	11	LAS-SP
GA	LOWNDES	LANGSDALE #1	HUNT OIL CO	5,052	50	LAS-SP	166	LAS-SP
GA	MITCHELL	J.H. Pullen No. 1	Stanolind Oil & Gas Co	7,487	385	LAS-SP	388	LAS-SP
GA	PIERCE	Adams-McCaskill No. 1	Pan American Petroleum Corp.	4,375	26	LAS-SP	4	LAS-SP
GA	SCREVEN	Helen H. Pryor No. 1	F.W. McCain	2,677	183	RASTER-SP	34	RASTER-SP
GA	Screven	MILLHAVEN TEST HOLE	USGS-DOE-GGS-GDNS	1,452	19	RASTER-GR		RASTER-GR
GA	SEMINOLE	Spindle Top 3	SEALY J R / C.E. Jack Prince	7,620	563	RASTER-SP	698	RASTER-SP
GA	STEWART	W. C. Bradley Co #1	W.O. Heinze & A.N. Spanel	2,916	122	LAS-SP	191	LAS-SP
GA	TELFAIR	Henry Spurlin #1	Parsons & Hoke	4,008	131	RASTER-SP	69	RASTER-SP
GA	TREUTLEN	JIM L GILLIS SR #1	BARNWELL DRLG CO INC	3,270	74	RASTER-SP	109	RASTER-SP
GA	TREUTLEN	Jim Gillis No. 1	McCain and Nicholson	3,253	111	RASTER-SP	190	RASTER-SP
GA	Washington	Malpasse SX 79 A- #1	Southeastern Exp.	5,641	100	LAS-GR	15	LAS-GR
GA	Washington	McCoy #1	SOUTHEASTERN EXPL. & PROD.	9,385	99	RASTER-GR	4	RASTER-GR
GA	Washington	SX 79 - Malpasse #1	Southeastern Exploration & Prod	2,576	31	RASTER-GR	0	RASTER-GR
GA	WAYNE	C.D. Hopkins et al. #1	DAVIS WILLIAM K	4,300	224	RASTER-GR	0	RASTER-GR
GA	WAYNE	Union Bag & Paper Co. No. 1	Humble Oil & Refining Co.	4,552	309	LAS-SP	42	LAS-SP
GA	WHEELER	MCRAE DB #1	SONAT EXPL INC	3,642	100	LAS-GR	45	LAS-GR
GA	Wheeler	Ronnie Towns #1	Southern Natural Gas Co.	4,075	227	LAS-SP	7	LAS-SP
GA	Wilkinson	Sepeco Hutton #1	Pan American	1,362	49	RASTER-SP+GR	5	RASTER-SP+GR
GA	Worth	Varner #1	J.D. Simmons, Inc.	4,200	351	RASTER-SP	241	RASTER-SP
SC	Barnwell	Savannah River Site #P5A / P-21	DOE	1,145	39	RASTER-GR	0	RASTER-GR
SC	BEAUFORT	HILTON HEAD TEST WELL #1	TOWN OF HILTON HEAD ISLAND	3,833	396	LAS-SP	108	LAS-SP
SC	Beaufort	Parris Island No. 2		3,454	109	RASTER-SP	3	RASTER-SP
SC	COLLETON	Norris Lightsey #1	ESSEX OIL & GAS CO	12,750	24	LAS-SP	0	LAS-SP
SC	Colleton	WATERBORO SHOTHOLE	USGS	2,213	0	RASTER-SP	78	RASTER-SP
SC	Dorchester	St. George No. 1	USGS	1,989	89	LAS-SP	16	LAS-SP
SC	Dorchester	Clubhouse Crossroads Corehole #1	USGS	2,598	70	RASTER-SP	19	RASTER-SP
SC	Florence	Lake City No. 34	USGS	918	35	RASTER-GR		RASTER-GR
SC	Jasper	SCDNR - DOE C-15	SCDNR	2,905	54	LAS-SP	91	LAS-SP

Table 2. Average porosity summations for wells used in study.					**TUSCALOOSA**		**PRE-TUSCALOOSA**	
State	**County**	**Well Label**	**Operator**	**TD**	**Average Porosity**	**Data Source**	**Average Porosity**	**Data Source**
AC	BRUNSWICK	913-1	GETTY OIL COMPANY	7,000	0.211	PHIS	0.206	PHIS
AC	BRUNSWICK	1005-1	TRANSCO EXPL&PROD CO	11,635	0.000	PHIS	0.180	PHIS
GA	CAMDEN	Pennington Union Camp #1	Amoco Production Company	10,000	0.240	PHIS		no sand
GA	Colquitt	H. Parker #1	Houston Oil & Minerals Corp.	6,902	0.319	PHIS	0.247	PHIS
GA	EARLY	Susie Wilson #1	EXXON CORPORATION	9,176	0.361	PHIS	0.333	PHIS
GA	Glynn	Union Camp Corp #1	William K. Davis	8,468	0.283	PHIS	0.261	PHIS
GA	JEFF DAVIS	J.L. Sinclair No. 1	Chevron USA, Inc.	4,063	0.267	PHID	0.237	PHID
GA	WAYNE	C.D. Hopkins et al. #1	DAVIS WILLIAM K	4,300	0.281	PHID		NFP
GA	WAYNE	Union Bag & Paper Co. No. 1	Humble Oil & Refining Co.	4,552	0.257	PHIS	0.220	PHIS
GA	WHEELER	MCRAE DB #1	SONAT EXPL INC	3,642	0.308	PHIS		NFP
GA	Wheeler	Ronnie Towns #1	Southern Natural Gas Co.	4,075	0.300	PHIS	0.245	PHIS
SC	BEAUFORT	HILTON HEAD TEST WELL #1	TOWN OF HILTON HEAD ISLAND	3,833	0.349	PHIX	0.120	PHIX
SC	COLLETON	Norris Lightsey #1	ESSEX OIL & GAS CO	12,750	0.083	PHIS		NFP
SC	Dorchester	St. George No. 1	USGS	1,989	0.183	PHID	0.232	PHID
SC	Jasper	SCDNR - DOE C-15	SCDNR	2,905	0.346	PHID	0.242	PHID

Map construction and definition of geologic sequestration units

We posted the results of Table 1 at their respective well locations and created isopach contour maps of net permeable sandstone. Likewise, for the isoporosity maps, we posted the results of Table 2 at their respective well locations and created isopach contour maps of average porosity. Interval isopach maps of both GSU's were made. First, the structure grid of a given unit's base was subtracted from the structure grid of the top. Second, Carr determined the interval isopach values from well control, again by subtracting top from base of the given interval. Finally, he used the 'grid' isopach Petra software utility to guide the contouring of the well control to ensure that the series of isopach maps and subsequent net sandstone isopach maps would be volumetrically valid.

After evaluating the cross sections (fig. 4) and preliminary maps, and supplementing the stratigraphic unit depth information from the many offshore geophysical studies (e.g. Dillon et al. (1979) map of top of Cretaceous from offshore reflection seismic surveys conducted during a series of cruises by, the U.S. Geological Survey and others), we selected three intervals to evaluate further. The approach was to identify top of "basement" (bottom of clastic sediments in which CO2 could be stored, which is defined later in report; fig. 4, plate 1) and top of Cretaceous (plate 2) horizons as upper and lower boundaries of potential geologic storage units. After many iterations of

correlation, we created gross isopach and net reservoir sandstone/limestone maps of the following major stratigraphic packages:

4. Pre-Tuscaloosa sandstones/conglomerates of undetermined Cretaceous to Triassic age
5. Tuscaloosa early Late Cretaceous (equivalents)
6. Post- Tuscaloosa sandstones and limestones of Late Cretaceous age

Table 3. Stratigraphic intervals of interest for geologic sequestration of CO2.

Geological Sequestration Unit (GSU)	**Approximate Geological Age**	**Lithology**	**Geographic Occurrence**	**Approximate Depth Range (ft)**	**Top / *Base***
Post-Tuscaloosa Upper Cretaceous*	Late Upper Cretaceous	carbonates (minor sandstone)	offshore continental shelf (OCS)	2,600-5,800	Upper Cretaceous / *Upper Tuscaloosa*
Tuscaloosa	Early Upper Cretaceous	sandstone	southern portion of coastal plain	2,600-4,500	Upper Tuscaloosa / *Base of Lower Tuscaloosa Sand*
Pre-Tuscaloosa	Lower Cretaceous, Upper Jurassic	sandstone	southwestern portion of coastal plain; OCS	2,600-11,000	Base of Lower Tuscaloosa Sand / *Basement*

* Not evaluated for CO_2 capacity in this report

Assuming typical subsurface pressure and temperature gradients, supercritical CO_2 can generally be stored at depths greater than 800 m (~2600 ft). This minimum sequestration depth is marked (red horizontal dashed line) on report cross sections A-A' and B-B' that are shown in figures 8 and 9 and plates 3 and 4. The thick cyan-colored line represents approximate Eagle Ford-age maximum flooding surface; Tuscaloosa and older sandstone bearing strata lie beneath it, and a mixture of sandstone and limestone bearing strata occur above it. The top of the Cretaceous is represented by the thick green unconformity line; top of the basement complex is shown by the thick dark purple unconformity line.

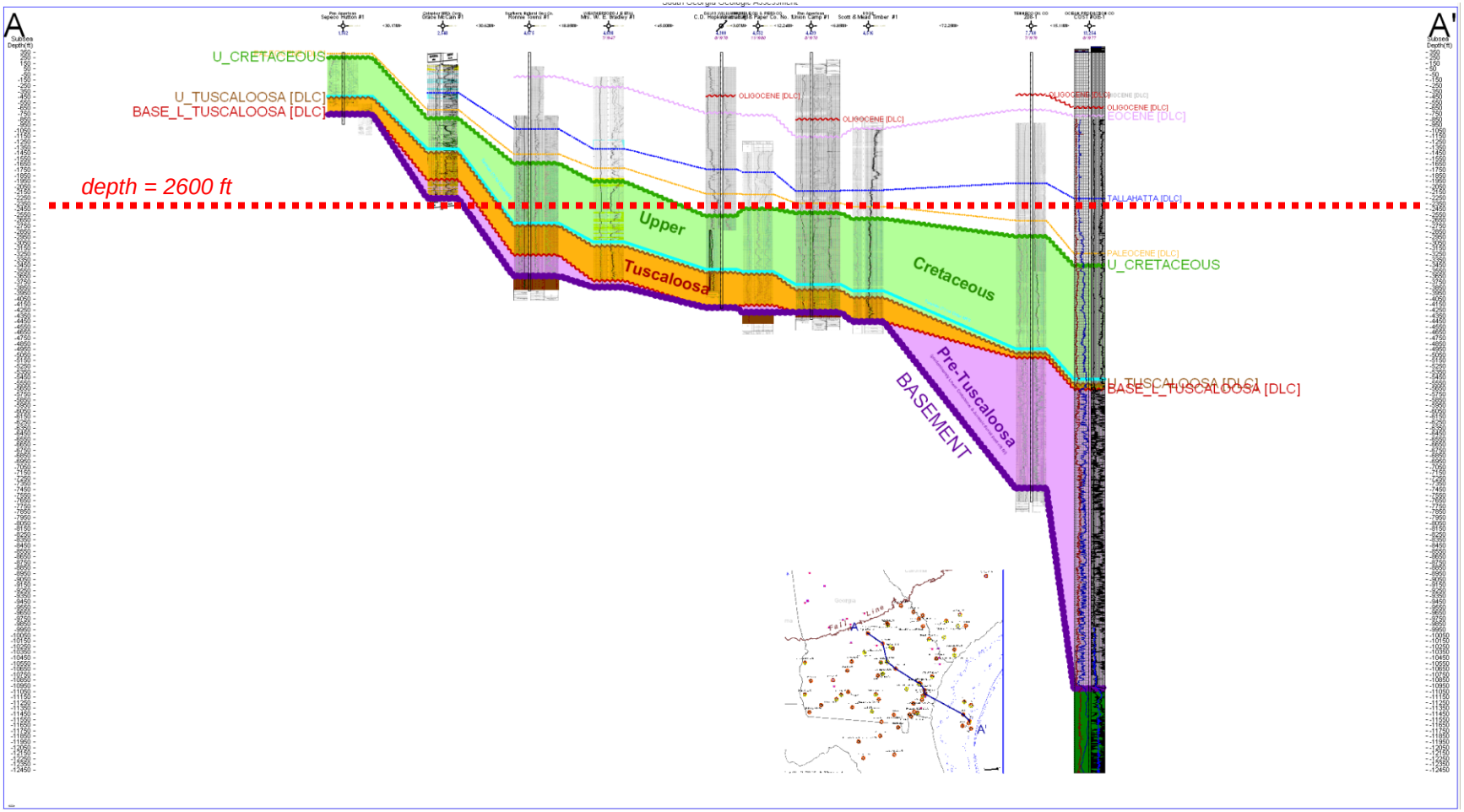

Figure 8. Structural cross section A-A'. NW to SE dip section from Fall Line to Federal OCS wells near continental shelf edge.

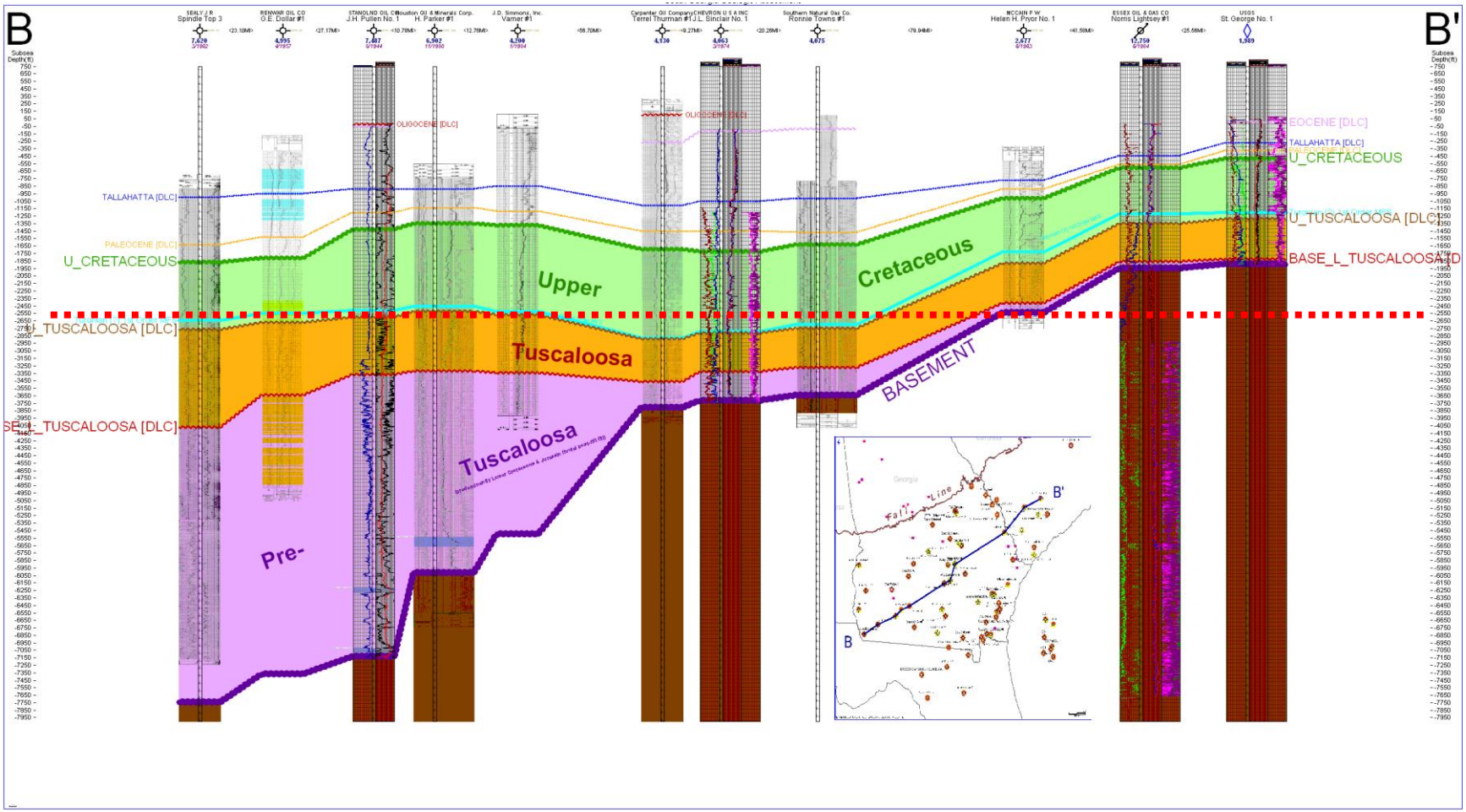

Figure 9. Structural cross section B-B'. NE to SW strike section from South Carolina border to Florida border

Inspection of the cross sections reveals that only two of the units have significant CO_2 sequestration potential (large unit thicknesses below 2,600 ft depth) in Georgia and the adjacent offshore. These are Pre-Tuscaloosa and Tuscaloosa GSU intervals. The upper Cretaceous Post-Tuscaloosa interval has sufficient thickness offshore (fig. 8), but there it is composed primarily of carbonate rocks. A map view of the areal extent of our two GSUs is shown by the red and brown polygons in figures 1 and 10. The extents of these polygons were defined by grid boundaries for the western and southern sides. The northern (updip) extent of each polygon was determined by where the depth below ground surface of the GSU is equal to 2,600 ft. Within the polygons each GSU interval appears at depths greater than 2, 600 ft. Extent of the eastern edge of GSUs was determined by where depth of seawater equals 400 m, which is approximately the edge of the continental shelf (figures 3, 10). It is not likely that drilling wells thousands of feet below the seafloor for offshore GS will take place in ocean water deeper than 400 m, or off the edge of the continental shelf in the near future. These same polygons are also shown on maps in subsequent sections (figures 11-19) where we provide results for each of GSUs.

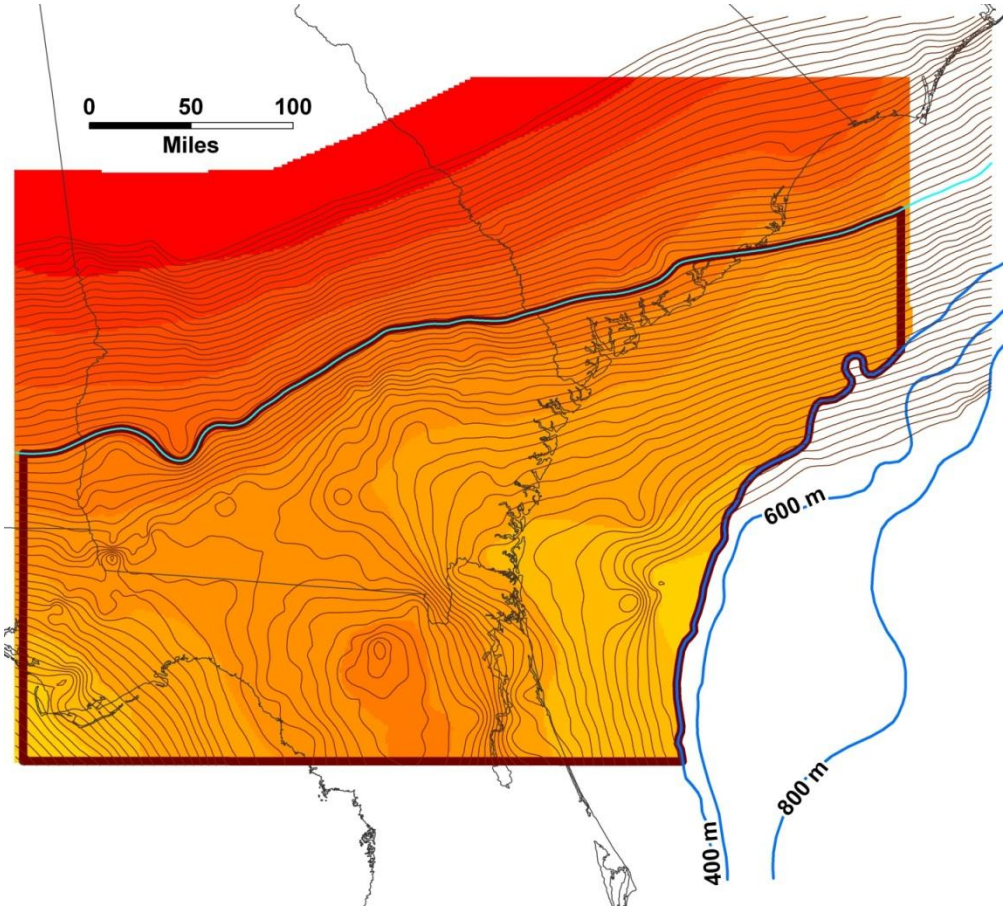

Figure 10. Graphical method used to select areal extent of geologic sequestration units. Brown lines are contours of top of Pre-Tuscaloosa GSU. The updip (northern) edge of this GSU corresponds to the 2,600 ft depth below surface contour line (light blue). The darker blue lines show water depth in the Atlantic Ocean.

Discussion and Results

Previous stratigraphic correlations of the Georgia coastal plain occurred primarily in response to oil exploration activity. After the 1943 discovery of Sunniland field in south Florida's Collier County, FL became an exploration target. Exploration moved northward to GA and deep tests there allowed study of cores, cuttings and geophysical logs. Significant contributions were made by Applin and Applin (1944; 1964; 1967) and Herrick (1961). These works focused primarily on paleontologic evaluation of well cuttings and the establishment of traditional time-rock units. Although no commercial oil was found in GA as a result of onshore drilling, exploration proceeded in the Atlantic offshore continental shelf from the late 1960's and accelerated during the 1970's.

Several broad stratigraphic studies were performed in advance of testing Georgia's Atlantic offshore continental shelf. The most notable works include Maher and Applin (1971), Brown et al. (1979), Gohn et al. (1980), and Kramer and Arden (1980). All of these authors provided cross sections of parts of the GA coastal plain, many of which provided useful guidance for this project, particularly those of Maher and Applin (1971) and Gohn et al. (1980). Published analyses of seismic and well data from late 1970's offshore oil exploration helped identify the major time-rock units and provided geophysical data enabling interpretations for linking Georgia's onshore and offshore strata (Buffler et al., 1978; Dillon et al., 1978, 1983; numerous references in Poag, 1978). Poppe et al.'s (1995) work providing facies and paleontologic interpretations of all Georgia's onshore deep tests was very useful to us, particularly in linking the pre-Tuscaloosa intervals in the offshore to the onshore of southwest Georgia.

In contrast to our approach, the previous works did not attempt to apply sequence stratigraphic concepts; nor were they as geographically expansive as these correlations, which link the GA coastal plain, parts of adjacent FL and SC, as well as the offshore continental shelf. Here we show the distribution and thicknesses of geologic units from "basement" up through the top of upper Cretaceous rocks within and between the deep sedimentary basins (western and eastern GA embayments) and out into the offshore Atlantic subseafloor. The stratigraphic interpretation presented in cross sections and maps are primarily based on Carr's correlation of geophysical logs, augmented with information from previously published reports. We use results of these interpretations to estimate capacity of the Pre-Tuscaloosa and Tuscaloosa GSUs.

Geologic basement units

"Basement" as used in this study refers to the shallowest appearance of crystalline rocks in geophysical logs (brown interval on cross sections in figures 8 and 9 and plates 3 and 4), or where log coverage is limited, acoustic basement defined by geophysical surveys (e.g. Buffler et al., 1978), and limited core data. Character of the basement differs in various regions of the study area. Crystalline metamorphic rocks like those exposed in the Piedmont physiographic province east of the Appalachian Mountains (fig. 1) underlie landward portions of the GA coastal plain (e.g., Dillon et al., 1978).

Pre-Cretaceous basement underlying the central GA uplift/FL Pennisular arch (Suwannee basin of others) (fig. 3) is composed of early Paleozoic (Ordovician, Silurian, and Devonian) sedimentary rocks that are underlain by felsic igneous rocks (granite and rhyolite) that are typical of continental crust. These rocks are thought to be fragments of Pangea left behind as the supercontinent began to break up during the Late Triassic approximately 200 million years ago. These Lower Paleozoic sandstones and shales are more similar to those found in northwest

Africa than those of North America (e.g., Aplin and Aplin, 1944; Smith, 1982; Milton, 1972; Milton, and Grasty, 1969; Heatherington and Mueller, 2003). The Pangean basement that underpins the Florida arch was also penetrated by the southernmost offshore Georgia wells.

In the rifted terrain of north central FL/southern GA/southern SC and offshore beneath the Atlantic seafloor (early Mesozoic rift basins on fig. 3), many wells have penetrated mafic igneous rocks (diabase and basalt) that are that more similar to oceanic than continental crust (Buffler et al., 1978; Dillon et al., 1978; Chowns and Williams, 1983). According to McBride et al. (1989), these mafic igneous rocks form an unconformity that separates underlying faulted early Mesozoic sediments from overlying later Mesozoic and Cenozoic coastal plain sediments, which are generally unfaulted. This unconformity, referred to as the J-reflector by Schilt et al. (1983), is thought to cover an ~10,000 km^2 area that extends from western GA to over 150 km offshore underneath the Atlantic continental shelf. A basalt sample taken from core collected near Charleston, SC and dated by Lanphere (1983) at 184 Ma (middle Jurassic) is assumed to be correlative with other mafic igneous rocks found at depth in GA. The idea is that during early Mesozoic continental rifting (stretching and tearing of the continental crust) mafic igneous rock flowed out over a large area much like that observed today on the Colorado Plateau of the western U.S.

It appears that previous researchers and practicing geologists frequently picked these mafic igneous rocks as basement. In fact, it appears that many wells "called TD" (i.e., ceased drilling) when "basement" was penetrated. Given that there probably few porous, permeable reservoirs beneath this zone, it was a reasonable assumption to define these early Mesozoic layered igneous strata as "economic basement" for the practical purpose of oil exploration and for this project. For onshore Georgia wells where basement was defined by the drill bit's first encounter with basalt or diabase, the basement structure contour map (fig. 11) probably represents a minimum estimate to depth of basement (Milton and Grasty, 1972; Barnett, 1975). The basement structure presented here (figs. 4, 11) represents depths to Piedmont, Paleozoic, and mafic igneous rocks contoured as a single surface. Black lines on fig. 11 are the same embayment central axes shown on fig. 3. Both of the GSUs are contained within upper Jurassic to early upper Cretaceous strata overlying basement rocks.

In the remaining sections we present details of the two GSUs defined herein, including structure contour maps of tops of the intervals, net sand isopach and iso-porosity maps. We also detail the approach and results of capacity estimates for these two GSUs.

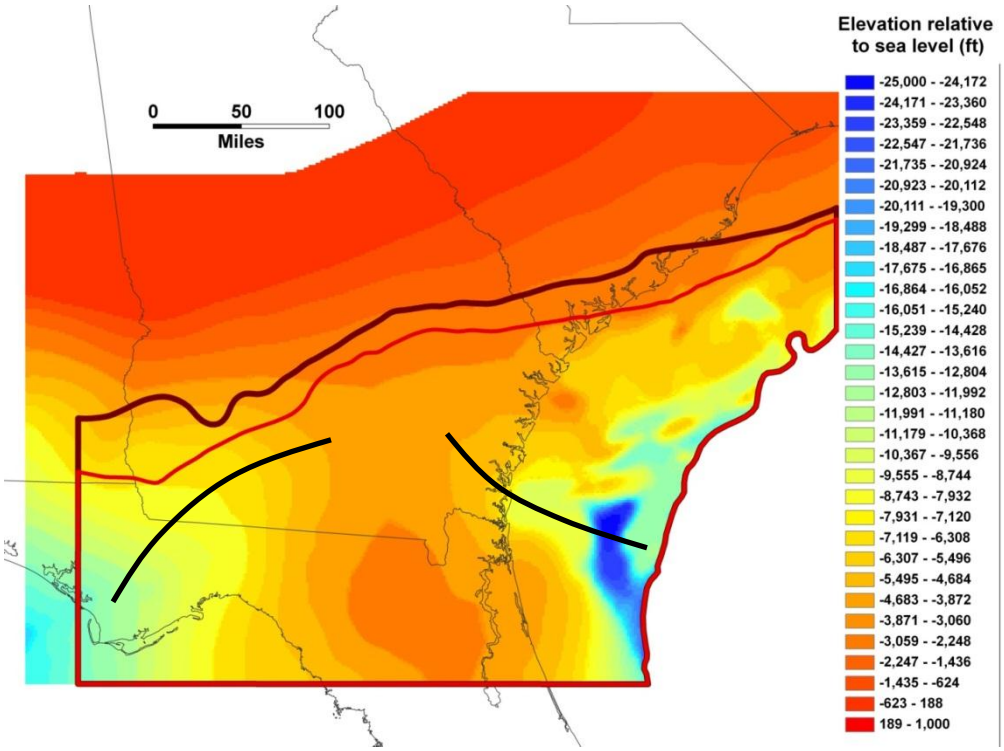

Figure 11. Geologic sequestration unit (GSU) areas superimposed on structure contour map of depth-to-basement-rocks. Red to orange depth range = 200-5,000 ft below sea level (bsl). Yellow to dark blue depth range = 5,000 to 25,000 ft bsl.

Geologic sequestration units

The two GSU intervals with sufficient thicknesses of net permeable clastic strata, at depths deep enough to store CO2 in supercritical phase, are Pre-Tuscaloosa and Tuscaloosa. Pre-Tuscaloosa GSU strata in which CO2 can be stored are sandstones and conglomerates of undetermined age (thought to be late Jurassic) to Cretaceous age. Strata of the Tuscaloosa GSU are primarily sandstones equivalent to Tuscaloosa Fm. strata of early upper Cretacous age. The surface footprints of these two vertically stacked intervals are shown for comparison as red and brown polygons in figures 1 and 11.

Pre-Tuscaloosa GSU

The base of the Pre-Tuscaloosa GSU is defined by the structure contour map on top of basement (figs. 4, 8, 9, and 11, plates 1, 2, and 3). The file names for geographic information system (GIS) shape files that accompany this report are BASEMENT STRUCTURE.* (.shp and associated files). The top of Pre-Tuscaloosa GSU is the base of the overlying Tuscaloosa Fm. (fig. 12) or time equivalent clastic deposits in southern GA and offshore below the Atlantic seafloor. The file names for geographic information system (GIS) shape files that accompany this report are BASE TUSCALOOSA STRUCTURE.* (.shp and associated files).

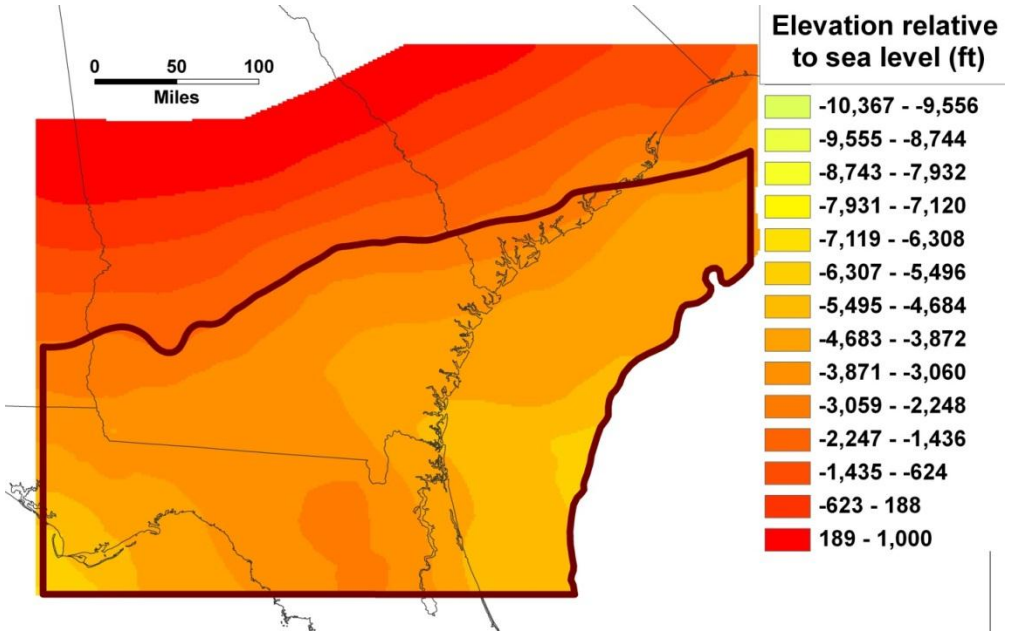

Figure 12. Structure contour map of base of lower Tuscaloosa Fm., which is the top of the Pre-Tuscaloosa GSU.

The top of the Pre-Tuscaloosa GSU ranges from ~2,400 ft below sea level (bsl) in the northwestern portion to 5,800 ft bsl on its eastern edge (fig. 12). The SE GA embayment axis in figs. 3 and 11 marks the deepest part of the embayment, which lies south of the zone of early Mesozoic rift basins. The vertical scale for top of Pre-Tuscaloosa structure is the same as in the basement map (figs. 4, 11) for comparison of the elevations. The entire embayment extends farther north roughly parallel to the Atlantic coastline (green and light blue shaded areas in fig. 11 and northeast corner of the GSU in fig. 12).

Correlation and mapping of the Pre-Tuscaloosa interval throughout the GSU (figs. 8, 9, 13 and plates 2, 3) allows us to show that net sands (1) thin over the Suwannee saddle, and (2) dramatically thicken in the SW and SE GA embayments. The full extent of this basin can also be seen in the Pre-Tuscaloosa net permeable isopach sand map (fig. 13). Here net sand thickness reaches a maximum of about 2, 500 ft in offshore portions of the GSU (figs. 8, 13). The other thick accumulation of net sand in the Pre-Tuscaloosa GSU corresponds to the location of the SW GA embayment (figs. 3, 13). Note that the top structure elevation patterns and the net sand thicknesses of the Pre-Tuscaloosa GSU mimic the basement structure. These patterns suggest that these two basins were subsiding relative to the central uplift areas in FL and GA during Pre-Tuscaloosa sediment deposition. The file names for geographic information system (GIS) shape files that accompany this report are PRETUSCALOOSA NETSAND.* (.shp and associated files).

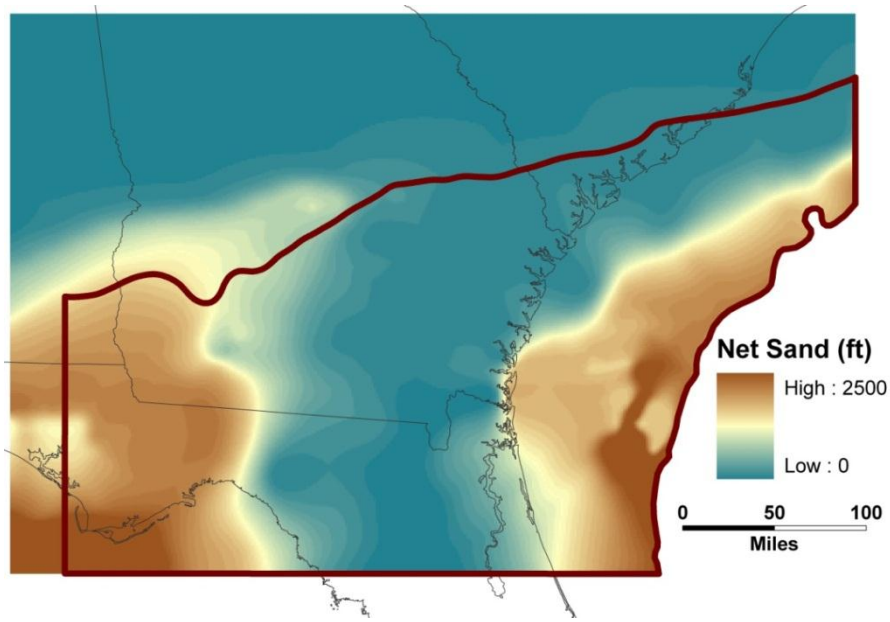

Figure 13. Pre-Tuscaloosa GSU net sand isopach map.

According to the porosity map of the Pre-Tuscaloosa GSU (fig. 14) generated in this study, strata in the SW GA embayment have higher porosity (darker blue areas) than those in the SE GA embayment. This apparent net sand thickening influences capacity estimates for this area as will be seen in the following section. The file names for geographic information system (GIS) shape files that accompany this report are PRETUSCALOOSA POROSITY.* (.shp and associated files).

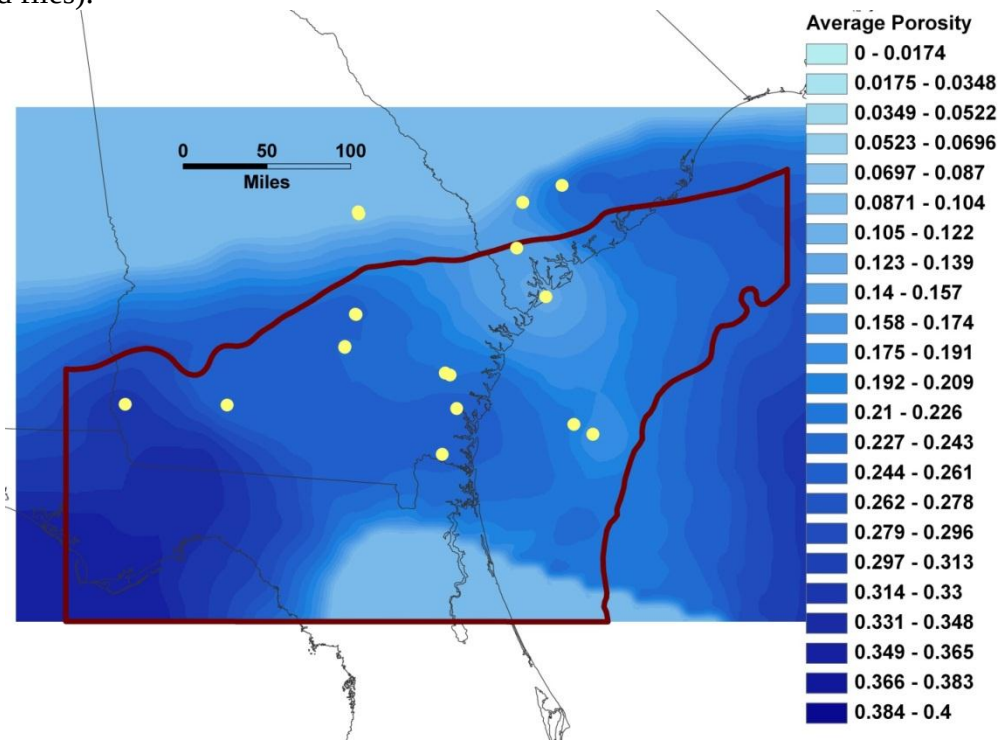

Figure 14. Pre-Tuscaloosa GSU porosity map. Yellow dots show locations of geophysical logs used to estimate porosity.

Tuscaloosa GSU

The base of the Tuscaloosa GSU is the structural top of the Pre-Tuscaloosa GSU (figs. 8, 9, 12). The structural top of this GSU corresponds to the top of the Tuscaloosa or time equivalent formations (figs. 8, 9, and 15, plates 2, 3). The vertical scale for top of Tuscaloosa structure is the same as in the basement and top of Pre-Tuscaloosa maps (figs. 4, 11, 12) for comparison of the elevations; the top of the Tuscaloosa GSU ranges from ~2,400 ft bsl to 5,600 bsl in offshore regions of the SE GA embayment. The file names for geographic information system (GIS) shape files that accompany this report are TOP TUSCALOOSA STRUCTURE.* (.shp and associated files).

Correlation and mapping of the Tuscaloosa throughout the GSU (figs. 8, 9, 15 and plates 2,3) allow us to show that suitable sand intervals (1) disappear from offshore portions of the SE GA embayment and (2) thicken slightly in the SW GA embayment. During Tuscaloosa time carbonate rocks were being deposited in the eastern, offshore portions of the SE GA embayment as sea level was rising relative to the continental margin (Frazier and Schwimmer, 1987). The structural surface of the basement, and the Pre-Tuscaloosa GSU as well, appear to have influenced the depositional patterns of sand within the Tuscaloosa GSU, at least within the SW GA embayment. For example see the large area of relatively thicker net sand on the western side of the Tuscaloosa GSU (fig. 16). However, total net sand in the Tuscaloosa GSU is much thinner (maximum thickness of 77 ft) than in the Pre-Tuscaloosa GSU (maximum thickness of 2, 500 ft). Also note that by early upper Cretaceous (Tuscaloosa) time the area of thickest permeable sands in eastern GA shifted onshore to the northwest (fig. 16) relative to an offshore location in the Pre-Tuscaloosa GSU (fig. 13). The file names for geographic information system (GIS) shape files that accompany this report are TUSCALOOSA NETSAND.* (.shp and associated files).

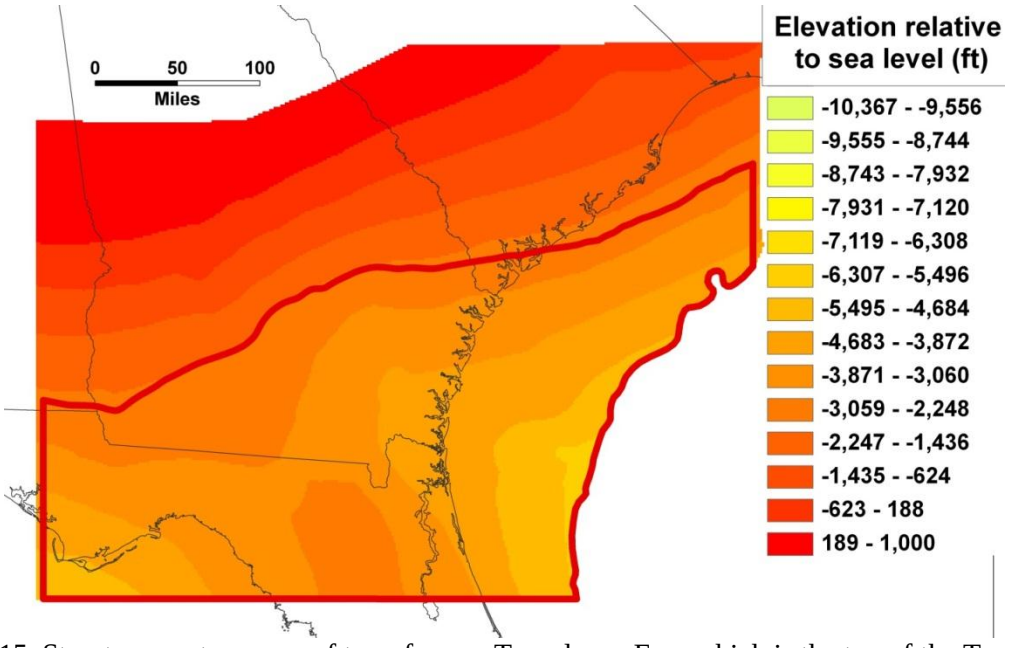

Figure 15. Structure contour map of top of upper Tuscaloosa Fm., which is the top of the Tuscaloosa GSU.

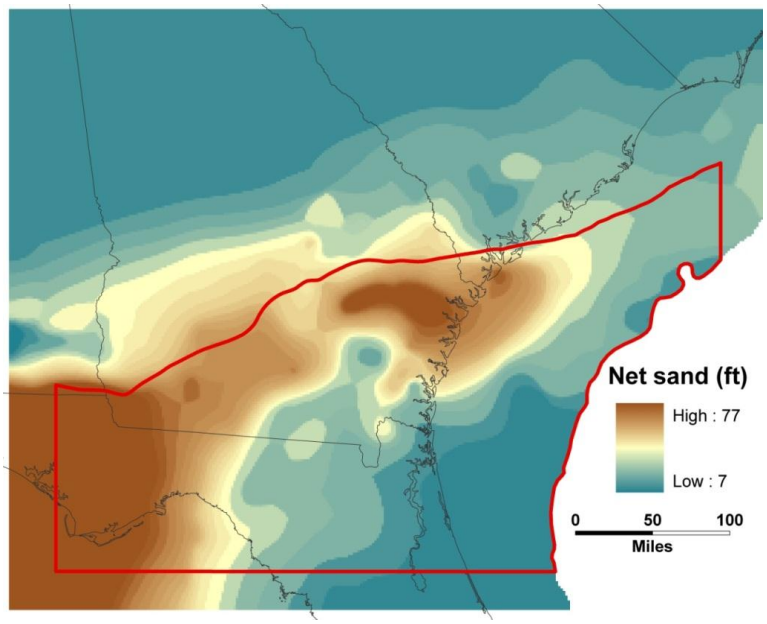

Figure 16. Tuscaloosa GSU net sand isopach map.

As in the Pre-Tuscaloosa GSU, the areas of highest porosity in the Tuscaloosa GSU (fig. 17) correspond spatially with the areas of thickest net sand (fig. 16). The file names for geographic information system (GIS) shape files that accompany this report are TUSCALOOSA POROSITY.* (.shp and associated files).

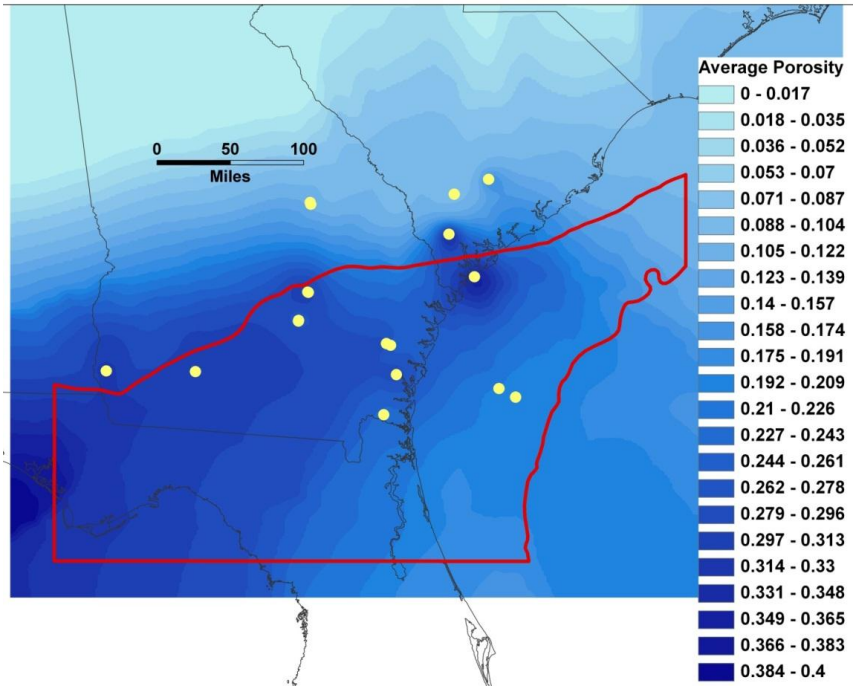

Figure 17. Tuscaloosa GSU porosity map. Yellow dots show locations of geophysical logs used to estimate porosity.

Capacity estimates

The methodology used to estimate CO2 storage capacity and the resulting capacity estimates for each of the two GSUs is described below. Estimates for the capacity of subsurface geologic units to store CO2 depend on the thickness of permeable sand present. After identifying units with enough permeable sand in locations appropriate for GS of CO2, we followed a series of additional steps to come up with the capacity estimations for the Pre-Tuscaloosa and Tuscaloosa GSUs. As previously detailed, the steps we took to select the GSUs included delineation of structural tops and bottoms, summation of net permeable sands, and estimation of porosity for each unit. All of this work was completed in IHS Petra© software and exported to Geographic Information Systems (GIS) shape files for further analysis using ESRI ArcGIS (ArcMap©) software.

Work completed in ArcMap for each GSU included:

- Interpolated Petra-generated depth, area, and thickness contours to generate Arc-grids (metric units)
- Adjusted depth below sea level grids (top and bottoms of units) to depth below surface for onshore areas by adding ground surface elevation (fig. 10)
- Defined GSU area polygons by (1) trimming northern edge of grid along 2, 600 ft (800 m) depth below ground surface contour, (2) trimming eastern edge along 400 m bathymetric contour, which approximates the seaward extent of the continental shelf (fig. 10).
- Calculated mid-point depths below ground surface for each grid cell within each polygon to use in CO2 density calculation. For the Pre-Tuscaloosa GSU this is the mid-point between the top of basement and the base of the Tuscaloosa Fm. For the Tuscaloosa GSU this is the mid-point between the top and bottom of the Tuscaloosa Fm.
- Interpolated Petra-generated net sand and porosity contours to generate Arc-grids
- Performed grid algebra within each 2.3 km^2 grid cell (number of grid cells within the Pre-Tuscaloosa GSU = 82,369; number of grid cells within the Tuscaloosa GSU = 72,314) using a formula that defines mass resource estimate potential of CO_2 in saline formations (MIT, 2010; NETL, 2010):

Eqn. 4. $$G_{CO2} = A_t \; h_g \; \phi_t \; \rho_{CO2} \; E_{saline}$$

Where:

G_{CO2} = mass of CO2 stored (kg)

A_t = geographical area defining region of CO_2 storage (m^2)

h_g = gross formation thickness (m)

ϕ_t = total porosity

ρ_{CO2} = density of CO_2 estimated at temperature and pressure of anticipated storage (reservoir) conditions (kg/m^3)

E_{saline} = CO_2 storage efficiency factor (we used E_{P50} = 0.02, and 0.004, 0.055)

We calculated CO2 density for each grid cell midpoint-depth using the Winprop© routine (an equation solver) within CMG (Computer Modeling Group LTD.) reservoir simulation software to solve the Peng-Robinson equation of state (Peng and Robinson, 1976). Simply stated, Peng-Robinson is an equation that calculates molar volume of a fluid at specified temperature and pressure, and also using other input values such as the universal gas constant, R, critical temperature, T_c, etc. Then by knowing the molecular mass of CO2, one can calculate the density because volume = mass/density. The steps taken to get to the point of solving for CO2 density included:

- Assigned a temperature for specific mid-point depths in GSUs assuming a surface temperature of 59 °F and a gradient of 1.5 F/100 ft (Griffin et al., 1969; Reel and Griffin, 1971), changing temperature every 30 ft
- Increased pressure with depth according to a hydrostatic pressure gradient of
- Calculated CO2 density for tabulated mid-point depths using the Peng-Robinson equation described above.
- Converted resulting density values in lb/ft^3 to kg/m^3 and interpolated to Arc-grid format.

Results of the capacity calculations (using **Eqn. 4**) for both the Pre-Tuscaloosa and Tuscaloosa GSUs are shown in figures 18 and 19, and table 4. The color scale for capacity is the same for both the Pre-Tuscaloosa and the Tuscaloosa GSUs (figs. 18, 19); thus it is more obvious that there is much higher capacity for GS of CO2 in the deeper Pre-Tuscaloosa than in the shallower Tuscaloosa GSU. In both images, grid cells shaded gray mark areas of zero capacity.

The total capacity for the Pre-Tuscaloosa GSU, using an efficiency factor (E) of 2 percent, is ~111 Gt over an area of ~74,000 mi^2 (191,000 km^2) (table 4). Capacity estimates for this unit over the same area using E = 0.4 and 5.5 percent are included in table 4. The maximum capacity (for E = 2 percent) within a single 2.3 km^2 grid cell in the underlying Pre-Tuscaloosa GSU is just over nine million tons (0.009 Gt); the highest capacity grid cells are shaded in blue (fig. 18). Note that areas with higher capacity (yellow-green-blue range) are in offshore portions of the SW and SE GA embayments (fig. 3), which is where the thickest accumulations of permeable sands and highest estimated porosities (e.g. figs. 13, 14) lie. We are most confident in capacity estimates for areas covered by the seven cross sections shown in fig. 4. The reason being that areas outside of those covered by the cross sections are outside of our area of geophysical log coverage (Recall this was discussed in detail in the Methodology section). So of the Pre-Tuscaloosa GSU areas with higher capacity, we are most confident in the onshore portions of the SW GA embayment, and SE GA embayment strata offshore below the Atlantic continental shelf. It makes sense that in central portions of the study area where post-rift sediments are thin, capacity estimates are low; this is the Suwannee saddle (FL/GA uplifts) area (figs. 3, 4, 11).

We are less confident in the Pre-Tuscaloosa GSU highest capacity estimates (blue shaded areas) offshore below the eastern Gulf of Mexico (GOM) continental shelf (fig.18), and consider results for this area to be only reconnaissance level. Using results for E = 2 percent, this ~4,600 km^2 area accounts for ~13 Gt of the total capacity estimate for the Pre-Tuscaloosa GSU. In other words, 2.4 percent of the Pre-Tuscaloosa area accounts for 12 percent of the capacity. However the area is worth including here, especially since results of other reconnaissance level studies have suggested that offshore portions of the SW GA embayment may contain large thicknesses of permeable sands (e.g. Mancini et al., 1987).

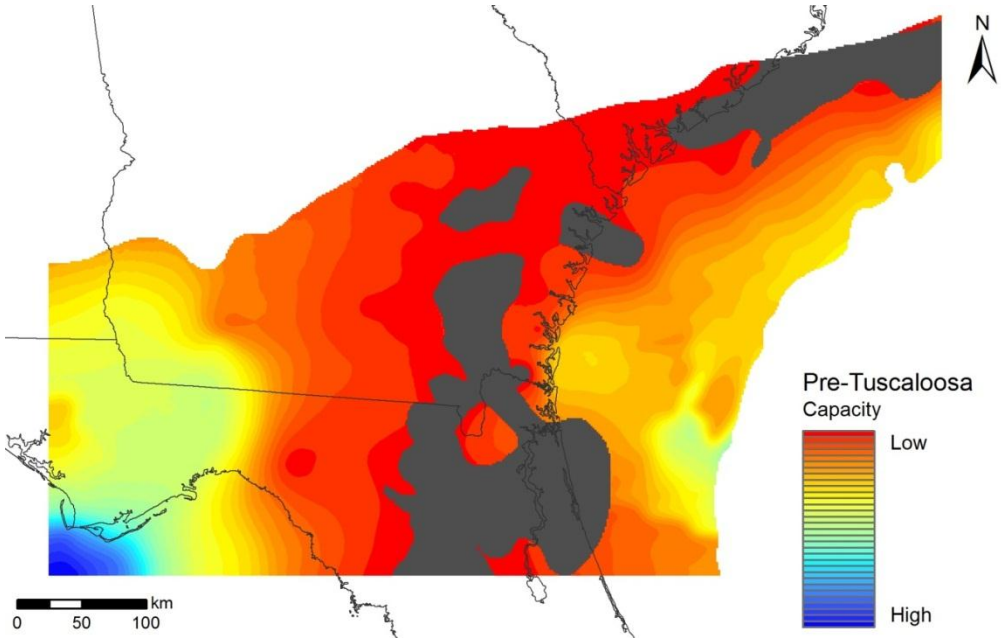

Figure 18. Pre-Tuscaloosa GSU capacity ranges from zero (gray areas) to over nine million tons (dark blue areas) per 0.9 mi^2 (2.3 km^2) grid cell using an efficiency factor (E) of two percent.

Table 4. Summary of capacity information for Pre-Tuscaloosa and Tuscaloosa GSUs.

	Tuscaloosa GSU	Pre-Tuscaloosa GSU
Area (mi^2)	64,892	73,915
Area (km^2)	168,070	191,440
for E = 0.02		
Mass (kg)	30,576,708,605,597	110,774,300,000,000
Mass (tonnes)	30,576,708,606	110,774,300,000
Mass (Gt)	31	111
for E = 0.004		
M (kg)	6,115,342,149,255	22,154,852,585,700
M (tonnes)	6,115,342,149	22,154,852,586
M (Gt)	6	22
for E = 0.055		
M (kg)	84,085,950,138,676	304,629,200,000,000
M (tonnes)	84,085,950,139	304,629,200,000
M (Gt)	84	305

The total capacity for GS of CO2 in the Tuscaloosa GSU, using E = 2 percent, is ~31 Gt over an area of ~65,000 mi^2 (168,000 km^2) (table 4). Capacity estimates for this unit over the same area using E = 0.4 and 5.5 percent are included in table 4. The maximum capacity within a single 2.3 km^2 cell in the overlying Tuscaloosa GSU, using E = 2 percent, is just over two million metric tons (0.002 Gt) (fig. 19). So the capacity for GS of CO2 in the Tuscaloosa GSU is only ~28 percent of that estimated for the Pre-Tuscaloosa GSU. As with the Pre-Tuscaloosa GSU, the highest capacity estimates fall within the SW GA embayment. In contrast to the Pre-Tuscaloosa results, most of the capacity in the Tuscaloosa GSU is onshore.

Reasons for differences in the distribution of capacity between the two GSUs are related to depositional processes taking place during the two respective geologic time periods. From middle Jurassic to lower Cretaceous time, nearshore deposition was dominantly continental clastic sediments with carbonate deposition being limited to areas farther offshore near the Blake Plateau. By upper Cretaceous time when sea level was rising, most of the rocks being deposited in the SE GA embayment were carbonates (Buffler et al., 1978; Frazier and Schwimmer, 1987). This pattern of deposition matches the results of net sand distribution documented herein.

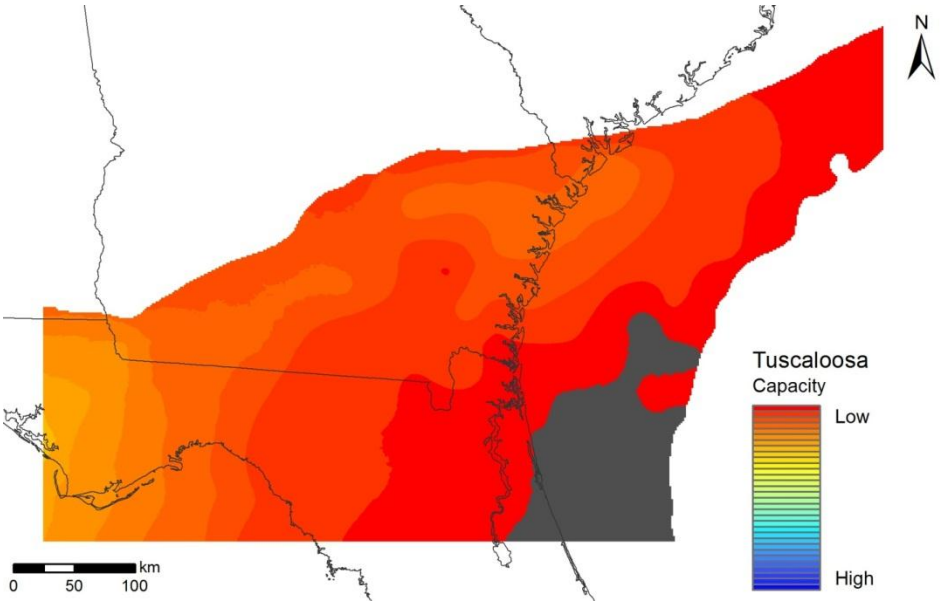

Figure 19. Tuscaloosa GSU capacity ranges from zero (gray areas) to over two million tons (yellow-orange areas) per 0.9 mi^2 (2.3 km^2) grid cell using an efficiency factor (E) of two percent.

Conclusions

This work surpasses the scope of previous individual studies through identification of two GSUs that span the GA coastal plain, parts of adjacent FL and SC, and extend out onto the offshore continental shelf of the Atlantic Ocean and a small area of the eastern Gulf of Mexico. Delineation of the subsurface geologic units was accomplished using sequence stratigraphic methods, which allow interpretations that should more accurately predict reservoir properties.

Even though the results presented here provide more accurate capacity estimates than previously calculated in the SE US (Smyth et al., 2008), they will still need to be refined by site-level investigations. The method for calculating capacity (MIT, 2010) is meant to be used for

regional assessments without refined estimates of specific intervals into which the CO2 will be injected. For example permeability is not considered so inter-well heterogeneity (connectedness of sands identified in individual wells) is not taken into account.

The potential to store CO2 in deep (greater than 2,600 ft) subsurface geologic strata underlying southern GA and offshore below the Atlantic seafloor is significant. Here we present two new geologic sequestration units (Pre-Tuscaloosa and Tuscaloosa) identified in this area that are capable of storing up to 15 giga tonnes (billon metric tons) (Gt) of CO2 within clastic sedimentary strata.

Previous estimates for areas surrounding and slightly overlapping our two new GSUs were based on limited and generalized data sets, which were primarily from research reports and published literature (Smyth et al., 2008). However given the information available, these previous estimates are still valid.

Maps and cross sections generated during this study are consistent with earlier research results in terms of (1) gross vertical and lateral distribution of major geologic strata and (2) patterns of deposition of sedimentary strata being controlled by the following regional structural features: Southwest Georgia Embayment, Southeast Georgia Embayment, and the
Central Georgia uplift/Florida Pennisular arch (referred to by some researchers as the Suwannee Saddle.

Operators of coal- and natural gas-fired power plants, and other types of industrial facilities, that release significant volumes CO2 to the atmosphere have options for GS in the SE US.

Acknowledgements

GCCC personnel thank the following power companies, Duke Energy, Santee Cooper Power, and Southern Company for support through the SSEB for primary funding of this project. We also appreciate supplementary funding received from the SECARB phase III National Carbon Sequestration Atlas program, and researcher-support from JSG.

References

Alberty, M., 1994, The influence of the borehole environment upon compressional sonic logs; *in* SPWLA 35th Annual Logging Symposium, June 19-22, 1994, 17 p.

Applin, P.L. and Applin, E.R., 1944, Regional subsurface stratigraphy and structure of Florida and southern Georgia, AAPG Bull. V. 28, no. 12, p. 1673-1723.

Applin, P.L., 1951, Preliminary report on buried pre-Mesozoic rocks in Florida and adjacent states. U.S.G.S. Circular 91, 28 p.

Applin, E.R. and P.L. Applin, 1964, Logs of selected wells in the coastal plain of Georgia, Georgia Survey Bulletin No. 74, 229 p.

Applin, P. L. and Applin, E. R., 1965, The Commanche Series and associated rocks in the subsurface in central and south Florida, US Geol. Surv. Prof. Pap. 447, 82 pp.

Applin, E.R. and P.L. Applin, 1967, The Gulf Series in the subsurface in northern Florida and southern Georgia, USGS Prof. Paper 524-G, 33 p.

Asquith, G. and D. Krygowski, 2004, Chapter 3, Gamma Ray, *in* Basic Well Log Analysis: AAPG Methods in Exploration 16, p. 31-35.

Barnett, R.S., 1975, Basement structure of Florida and its tectonic implications, Gulf Coast Assoc. Geol. Soc. Trans., v XXV, p. 122-142.

Buffler, R. T., Watkins, J.S., and Dillon, W.P., 1979, Geology of the offshore southeast Georgia embayment, U.S. Atlantic Continental Margin, Based on multichannel seismic reflection profiles: American Association of Petroleum Geologists Memoir 29, p. 11-41.

Chowns, T. M., and Williams, C. T., 1983, Pre-Cretaceous rocks beneath the Georgia coastal plain – regional implications *in* Gohn, G., ed., Studies related to the Charleston, SC earthquake of 1886 – tectonics and seismicity: U.S.G.S. prof. paper no. 1313, L1-L42.

Clavier, C., et al 1984 Theoretical and Experimental Bases for the Dual-Water Model for Interpretation of Shaly Sands, SPEJ vol. 21, No., pp. 153-168.

Clavier, C., W.R. Hoyle and D. Meunier, 1971. Quantitative interpretation of TDT logs; Part I and II,
Journal of Petroleum Technology, (6): 743-763. Colorado, D.W. Hilichie, Inc.

Dalziel, I. W. D., 1995, Earth before Pangea, Scientific American, 272(1): 58-63.

Dalziel, I.W.D., Mosher, S., and Gahagan, L.M., 2000, Laurentia-Kalahari collision and the assembly of Rodinia, Journal of Geology, vol. 108, p. 499-513.

Dalziel, I.W.D., 2000, Texas Through Time, The University of Texas at Austin Discovery magazine, vol. 15(3), p. 12-17.

Dalziel, I.W.D., 1997, Overview: Neoproterozoic-Paleozoic geography and tectonics: Review, hypothesis, environmental speculation , Geological Society of America Bulletin, vol. 109(1), pp. 16-42.

Dillon, W.P., Paull, C.K., Buffler, R.T., and Fail, J-P., 1978, Structure and development of the Southeast Georgia embayment and northern Blake Plateau: preliminary analysis: American Association of Petroleum Geologists Memoir 29, p.27-41.

Dillon, W. P., K. D. Klitgord, and C. K. Paull, 1983, Mesozoic development and structure of the continental margin off South Carolina, in G. S. Gohn, ed., Studies related to the Charleston, South Carolina, earthquake of 1886—tectonics and seismicity: Geological Survey Professional Paper 1313, p. N1–N16.

Fenneman, N. M., and Johnson, D. W., 1946, Physical divisions of the United States: USGS map, scale: 1:7,000,000.

Frazier, W.J. and Schwimmer, D.R., 1987, Regional stratigraphy of North America: Plenum Press, New York and London, 719p.

Gohn, G.S., 1992, Revised nomenclature, definitions, and correlations for the Cretaceous formations in USGS-Clubhouse Crossroads #1, Dorchester County, South Carolina: U.S. Geological Survey Professional Paper 1518, 39 p.

Gohn, G.S., and Campbell, B.G., 1991, Recent revisions to the stratigraphy of subsurface Cretaceous sediments in the Charleston, South Carolina, area: South Carolina Geology, v. 34, n. 1-2, p. 25-38.

Gohn, G. S., Smith, C. C., Christopher, R. A., and Owens, J. P., 1980, Preliminary cross sections of Cretaceous sediments along Georgia coastal margin: U.S. Geological Survey Miscellaneous Field Studies Map MF -1015-C, 2 sheets.

Gohn, G. S., Higgins, B. B., Smith, C. C., and Owens, J. P., 1977, Lithostratigraphy of the deep corehole (Clubhouse Crossroads corehole 1) near Charleston, South Carolina: Studies related to the Charleston, South Carolina, earthquake of 1886; a preliminary report, U. S. Geological Survey Professional Paper 1028, p. 59-70.

Griffin, G.M., Therick, P.A., Reel, D.A., and J.P. Manker, 1969, Geothermal Gradients in Florida and Southern Georgia, GCAGS Trans, v. 19, p.189-193.

Heatherington, A.L. and P.A. Mueller, 2003, Mesozoic igneous activity in the Suwannee Terrane, southeaster USA: Petrogenesis and Gondwanan affinities, Gondwana Research, v. 6, p. 296-311.

Herrick, S.M., 1961, Well logs of the coastal plain of Georgia, Georgia Survey Bulletin No. 70, 462 p.

Hovorka S.D., C. Doughty, S.M. Benson, B.M. Freifeld, S. Sakurai, T.M. Daley, Y.K. Kharaka, M.H. Holtz, R.C. Trautz, H.S. Nance, L.R. Myer and K.G. Knauss. 2006. "Measuring Permanence of CO_2 Storage in Saline Formations: The Frio Experiment." *Environmental Geosciences* 13(2):105-121.

Hovorka S.D., 2006, "Frio Brine Storage Experiment—Lessons Learned." In *8th International Conference on Greenhouse Gas Control Technologies*, 6 pp. Trondheim, Norway.

Hovorka, S. D., Doughty, C., Benson, S. M., Pruess, K., and Knox, P. R., 2004, The impact of geological heterogeneity on CO_2 storage in brine formations; a case study from the Texas Gulf Coast, In: Baines, S. J. and Worden, R. H., eds., Geological storage of carbon dioxide, Geological Society Special Publications, V. 233: 147-163.

Hovorka, S. D., Romero, M. L., Treviño, R. H., Warne, A. G., Ambrose, W. A., Knox, P. R., and Tremblay, T. A., 2000, Project evaluation: phase II: optimal geological environments for carbon dioxide disposal in brine-bearing formations (aquifers) in the United States: The University of Texas at Austin, Bureau of Economic Geology, final report prepared for U.S. Department of Energy, National Energy Technology Laboratory, under contract no. DE-AC26-98FT40417, 222 p.

King, P. B., 1959, The Evolution of North America: Princeton University Press, 197p., 1 plate.

Klitgord, K. D., and Behrendt, J. C., 1979, Basin structure of the U. S. Atlantic margin, in: Watkins, J. S., and Dickerson, P. W., eds., Geological and geophysical investigations of continental margins, American Association of Petroleum Geologists Memoir 29: 85-112.

Lanphere, M.A., 1983, $^{40}Ar/^{39}Ar$ ages basalt from Clubhouse Crossroads test hole #2 near Charleston, South Carolina *in* Gohn, G.S. (ed.), Studies related to the Charleston, South Carolina earthquake of 1886 – tectonics and seismicity: USGS PP 1313, p. B1-B8.

Litynski, J., Deel, D., Rodosta, T., Guthrie, G., Goodman, A., Hakala, A., Bromhal, G., Frailey, S., 2010, Summary for the methodology for development of geologic storage estimates for carbon dioxide, Appendix B *in* 2010 Carbon Sequestration Atlas of the United States and Canada: Department of Energy National Energy Technology Laboratory, p. 136-152.

Mancini, E. A., Mink, R. M., Payton, J. W., and Bearden, B. L., 1987, Environments of deposition and petroleum geology of the Tuscaloosa Group (Upper Cretaceous), South Carlton and Pollard Fields, southwestern Alabama: AAPG Bulletin, v. 71, p. 1128–1142.

McBride, J.H., K.D. Nelson and L.D. Brown, 1989, Evidence and implications of an extensive early Mesozoic rift basin and basalt-diabase sequence beneath the southeast coastal plain, Geol. Soc. America Bull., v. 101, p. 512-520.

Milton, C., 1972, Igneous and metamorphic basement rocks of Florida, Fla. Bur. Geol., Bull. No. 55, 125 p.

Milton, C. and Grasty, R., 1969, Basement rocks of Florida and Georgia. Amer. Assoc. Petr. Geol. Bull., v. 53, p. 2483-2493.

MIT, 2010, Draft Report: Method from Methodology for Development of Geologic Storage Potential for Carbon Dioxide, U.S. DOE/NETL Carbon Sequestration Program.

Nelson, K.D., J. A. Arnow, J. H. McBride, J. H. Willemin, J. Huang, L. Zheng, J. E. Oliver, L. D. Brown, and S. Kaufman, 1985, New COCORP profiling in the southeastern United States. Part I: Late Paleozoic suture and Mesozoic rift basin: *Geology:* Vol. 13, No. 10, pp. 714–718.

NOAA, 2006, National Geophysical Data Center: www.ngdc.noaa.gov/mgg/topo/ globe.html

Olsen, P. E., Froelich, A. J., Daniels, D. L., Smoot, J. P., and Gore, P. J. W., 1991, Rift basins of

early Mesozoic age, *in* Horton, J. W., Jr. and Zullo, V. A., eds., The Geology of the Carolinas: Carolina Geological Society Fiftieth Anniversary Volume: Knoxville, The University of Tennessee Press, p. 142–170.

Peng, D.Y. and Robinson, D.B., 1976. Ind. Eng. Chem. Fund., v. 15, p. 59.

Popenoe, P. and Zietz, I., 1977, The nature of the geophysical basement beneath the Coastal Plain of South Carolina and northeastern Georgia, U.S. Geological Survey Professional Paper 1028, p. 119-137.

Poppe, L.J., Popenoe, P., Poag, C., Swift, B., 1995, Stratigraphic and paleoenvironmental summary of the southeast Georgia embayment - a correlation of exploratory wells: Marine and Petroleum Geology, v. 12, no. 6. p.
677-690.

Raymer, L.L., Hunt, E.R., and Gardner, J.S., 1980, An improved sonic transit time-to-porosity transform: SPWLA 21 Ann. Logging Symp., July 8-11, 1980, 1-12.

Reel, D.A and Griffin, G.M., 1971, Potentially petroliferous trends in Florida defined by geothermal gradients, GCAGS Trans, v. 21, p.31-36.

Schlumberger, 1998, Chapter 3, Spontaneous Potential and Natural Gamma Ray Logs, in: Log Interpretation Principles/Applications, Schlumberger Wireline & Testing, Sugar Land, Texas.

Schilt, F.S., Brown L.D., Oliver, J.E., and Kaufman, S., 1983; Subsurface structure near Charleston, South Carolina: Results of COCORP reflection profiling in the Atlantic Coastal Plain, *in* Gohn, G.S., ed., Studies related to the Charleston, SC earthquake of 1886- Tectonics and seismicity: U.S.G.S. Prof. Paper 1313, p. H1-H19.

Scripps, 2006, Satellite Geodesy Web page: http://topex.ucsd.edu/WWW_html/ srtm30_plus.html

Smith, D.L., 1982, Review of the tectonic history of Florida basement, Tectonophysics, v. 88, p. 1-22.

UTIG, 2011, Plates project website: http://www.ig.utexas.edu/research/projects/plates/

Wyllie, M.R.J., Gregory, A.R., and Gardner, L.W., 1956, Elastic wave velocities in heterogeneous and porous media: Geophysics, 21, 41-70.

Wyllie, M.R.J., Gregory, A.R., and Gardner, G.H.F., 1958, An experimental investigation of factors affecting elastic wave velocities in porous media: Geophysics, 23, 459-493.